U.S. Department of Transportation

Federal Railroad Administration

Prototype Design of a Collision Protection System for Cab Car Engineers—Fabrication and Test

Office of Research, Development, and Technology
Washington, DC 20590

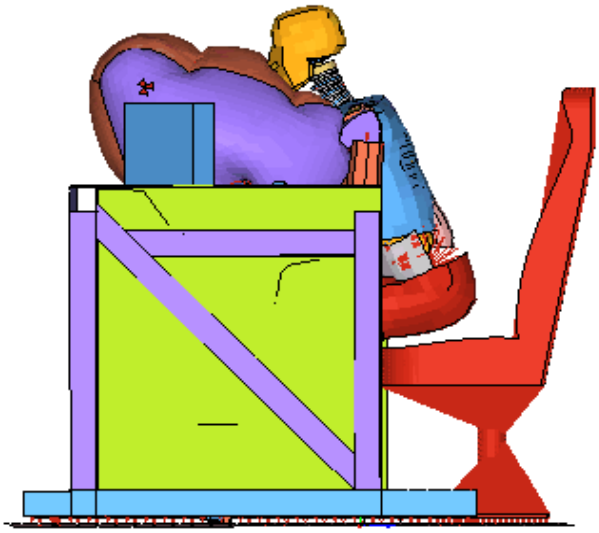

DOT/FRA/ORD-15/20

Final Report
June 2015

REPORT DOCUMENTATION PAGE

Form Approved
OMB No. 0704-0188

1. AGENCY USE ONLY (Leave blank)	2. REPORT DATE	3. REPORT TYPE AND DATES COVERED
	June 2015	Final Report, May 2012 – April 2013

4. TITLE AND SUBTITLE
Prototype Design of a Collision Protection System for Cab Car Engineers—Fabrication and Test

5. FUNDING NUMBERS

6. AUTHOR(S)
Anand Prabhakaran, Som P. Singh, and Anand R. Vithani

7. PERFORMING ORGANIZATION NAME(S) AND ADDRESS(ES)
Sharma & Associates, Inc.
100 W Plainfield Road
Countryside, IL 60525

8. PERFORMING ORGANIZATION REPORT NUMBER

9. SPONSORING/MONITORING AGENCY NAME(S) AND ADDRESS(ES)
U.S. Department of Transportation
Federal Railroad Administration
Office of Railroad Policy and Development
Office of Research and Development
Washington, DC 20590

10. SPONSORING/MONITORING AGENCY REPORT NUMBER
DOT/FRA/ORD-15/20

11. SUPPLEMENTARY NOTES
U.S. Department of Transportation
Research and Innovative Technology Administration
John A. Volpe National Transportation Systems Center
55 Broadway, Cambridge, MA 02142-1093

12a. DISTRIBUTION/AVAILABILITY STATEMENT
This document is available to the public through the FRA Web site at http://www.fra.dot.gov.

12b. DISTRIBUTION CODE

13. ABSTRACT (Maximum 200 words)

Advancements in the structural crashworthiness of passenger rail cars now make it possible to preserve the compartmentalized space occupied by a cab car engineer during a train collision. In order to translate this additional protection into improved survivability and mitigate injuries, it is necessary to protect the engineer from secondary impacts in such accident scenarios. Prior work on this issue resulted in the design of a conceptual Engineer Protection System (EPS) that could protect an engineer under moderate-to-severe frontal impact conditions.

The performance of this prototype EPS, which consists of an airbag and a deformable knee bolster system, was successfully demonstrated under simulated collision conditions, using a dynamic sled test for a 95^{th} percentile anthropomorphic test device (ATD). The test highlighted the ability of the EPS to protect a cab car engineer in a moderate-to-severe train collision, meeting all design criteria, including compartmentalization and limits of injury to the head, neck, chest, and femur, and continuing to the meet all functional requirements. The system functions without requiring input from the engineer, without restraining him or her, and without impeding egress, while adding minimally to cost or weight of the car.

14. SUBJECT TERMS
Crashworthiness, cab console, secondary impact protection, airbags, energy absorption, crushable knee bolster, sled testing, crash energy management, injury indices, finite element analysis

15. NUMBER OF PAGES
61

16. PRICE CODE

17. SECURITY CLASSIFICATION OF REPORT	18. SECURITY CLASSIFICATION OF THIS PAGE	19. SECURITY CLASSIFICATION OF ABSTRACT	20. LIMITATION OF ABSTRACT
Unclassified	Unclassified	Unclassified	

NSN 7540-01-280-5500
Standard Form 298 (Rev. 2-89)
Prescribed by ANSI Std. 239-18
298-102

METRIC/ENGLISH CONVERSION FACTORS

ENGLISH TO METRIC	METRIC TO ENGLISH
LENGTH (APPROXIMATE)	**LENGTH (APPROXIMATE)**
1 inch (in) = 2.5 centimeters (cm)	1 millimeter (mm) = 0.04 inch (in)
1 foot (ft) = 30 centimeters (cm)	1 centimeter (cm) = 0.4 inch (in)
1 yard (yd) = 0.9 meter (m)	1 meter (m) = 3.3 feet (ft)
1 mile (mi) = 1.6 kilometers (km)	1 meter (m) = 1.1 yards (yd)
	1 kilometer (km) = 0.6 mile (mi)
AREA (APPROXIMATE)	**AREA (APPROXIMATE)**
1 square inch (sq in, in^2) = 6.5 square centimeters (cm^2)	1 square centimeter (cm^2) = 0.16 square inch (sq in, in^2)
1 square foot (sq ft, ft^2) = 0.09 square meter (m^2)	1 square meter (m^2) = 1.2 square yards (sq yd, yd^2)
1 square yard (sq yd, yd^2) = 0.8 square meter (m^2)	1 square kilometer (km^2) = 0.4 square mile (sq mi, mi^2)
1 square mile (sq mi, mi^2) = 2.6 square kilometers (km^2)	10,000 square meters (m^2) = 1 hectare (ha) = 2.5 acres
1 acre = 0.4 hectare (he) = 4,000 square meters (m^2)	
MASS - WEIGHT (APPROXIMATE)	**MASS - WEIGHT (APPROXIMATE)**
1 ounce (oz) = 28 grams (gm)	1 gram (gm) = 0.036 ounce (oz)
1 pound (lb) = 0.45 kilogram (kg)	1 kilogram (kg) = 2.2 pounds (lb)
1 short ton = 2,000 pounds (lb) = 0.9 tonne (t)	1 tonne (t) = 1,000 kilograms (kg) = 1.1 short tons
VOLUME (APPROXIMATE)	**VOLUME (APPROXIMATE)**
1 teaspoon (tsp) = 5 milliliters (ml)	1 milliliter (ml) = 0.03 fluid ounce (fl oz)
1 tablespoon (tbsp) = 15 milliliters (ml)	1 liter (l) = 2.1 pints (pt)
1 fluid ounce (fl oz) = 30 milliliters (ml)	1 liter (l) = 1.06 quarts (qt)
1 cup (c) = 0.24 liter (l)	1 liter (l) = 0.26 gallon (gal)
1 pint (pt) = 0.47 liter (l)	
1 quart (qt) = 0.96 liter (l)	
1 gallon (gal) = 3.8 liters (l)	
1 cubic foot (cu ft, ft^3) = 0.03 cubic meter (m^3)	1 cubic meter (m^3) = 36 cubic feet (cu ft, ft^3)
1 cubic yard (cu yd, yd^3) = 0.76 cubic meter (m^3)	1 cubic meter (m^3) = 1.3 cubic yards (cu yd, yd^3)
TEMPERATURE (EXACT)	**TEMPERATURE (EXACT)**
[(x-32)(5/9)] °F = y °C	[(9/5) y + 32] °C = x °F

QUICK INCH - CENTIMETER LENGTH CONVERSION

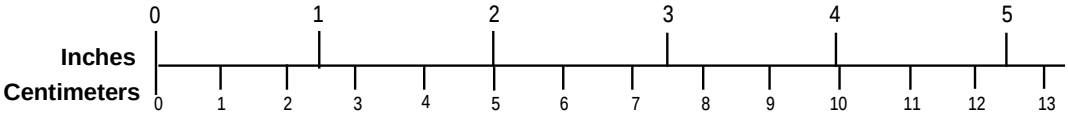

QUICK FAHRENHEIT - CELSIUS TEMPERATURE CONVERSIO

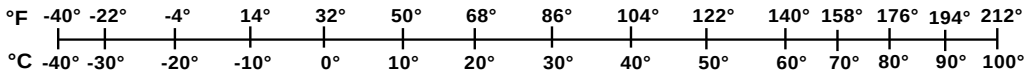

For more exact and or other conversion factors, see NIST Miscellaneous Publication 286, Units of Weights and Measures. Price $2.50 SD Catalog No. C13 10286

Updated 6/17/98

Acknowledgements

This work was sponsored by the Equipment Safety Research Program of the Federal Railroad Administration's Office of Research and Development. The authors are grateful for the support of Mr. Kevin Kesler, Chief of the Rolling Stock Division, and Mr. Jeff Gordon, Program Manager for the Passenger Equipment Safety Research Program.

The authors express their sincere appreciation and gratitude to Ms. Kristine Severson (Volpe Center), who served as the technical monitor and whose invaluable support, guidance, and patience were critical to the success of this project. The authors are also grateful for the guidance provided by Dr. Benjamin Perlman of the Volpe National Transportation Systems Center and Ms. Michelle Muhlanger, FRA Region 2 Deputy Regional Administrator, over the course of this project.

The authors also acknowledge the technical support provided by John Wallner, Soonsik Kim, and their team at Key Safety Systems, as well as Phillip Kosarek and his team at Altair Engineering. The authors are also grateful to Mr. Telis Kakaris and SCRRA/Metrolink for graciously donating a seat for this test effort.

Contents

Illustrations

Tables

Executive Summary

The performance of a prototype Engineer Protection System (EPS), which consists of an airbag system and a deformable knee bolster system, for cab cars (i.e. passenger rail cars with a compartment from which an engineer operates the train) was successfully demonstrated under simulated collision conditions, using a dynamic sled test. The test highlighted the ability of the EPS to protect a cab car engineer in a moderate-to-severe train collision, meeting all design criteria, including compartmentalization and limits of injury to the head, neck, chest, and femur, and continuing to meet all functional requirements. The system functions without requiring input from the engineer, without restraining him or her, and without impeding egress, while adding only minimally to cost or weight of the car.

Advancements in the structural crashworthiness of passenger rail cars now make it possible to preserve the space occupied by an engineer during a train collision, particularly in a cab car at the leading end of a train. In order to translate this additional protection into improved survivability and mitigate injuries, it is necessary to protect the engineer from secondary impacts in such accident scenarios.

Prior work on this project resulted in the design of a conceptual EPS that could protect an engineer under moderate-to-severe frontal impact conditions, similar to the conditions observed in prior, full scale passenger train tests conducted by the Federal Railroad Administration (FRA). This effort also established through simulations that, in the absence of a protection system (base case), such a collision event was not survivable based on the calculated high injury indices and lack of compartmentalization [1].

As part of this phase, Sharma & Associates, Inc. (SA) constructed:

- a baseline cab desk, which would serve as the test bed for the EPS
- the airbag subsystem, comprised of an airbag/cushion, an inflator, and assorted electronics
- the knee bolster subsystem, comprised of deformable brackets and honeycomb blocks

The EPS subsystems were then assembled into the baseline cab desk, and the full system was dynamically tested under a 23g EPS test pulse. The initial test showed that the prototype system met all specified safety criteria for the head, the chest, and the femurs, but that two of the six injury criteria for the neck were above targeted limits.

Subsequently, several alternatives for improving neck injury performance were studied, with a particular focus on airbag fold and tether length changes. Multiple airbag fold variations were evaluated using static deployment tests (i.e., the test sled is stationary, and the deployment sequence of the airbag is studied using high speed videography). Based on these test results, an alternative airbag design that consisted of reduced tether lengths with a ‘reverse roll’ fold pattern was selected for the second sled test.

All compartmentalization requirements and injury criteria, including those for the neck, were comfortably met during the second dynamic sled test with the alternate airbag configuration.

Subsequently, the test results were analyzed in detail to determine any differences between analytical model predictions and physical test results, and the analytical model was updated to better reflect the test results.
The measured injury criteria and target limits are outlined in the following table, along with additional information on what the values would have been in the absence of a protection system.

Table 1. Performance of the EPS

Injury Parameter	Index Limit	Injury Indices	
		Simulated Base Case (No protection)	Dynamic Sled Test with EPS
HIC_{15}	700	9,661	144
Chest 3ms (G)	60	38	32
Femur Left (N)	10,000	20,307	8,426
Femur Right (N)	10,000	20,236	8,996
Neck Tension (N)	4,170	5,089	1,951
Neck Compression (N)	4,000	2,525	1,200
N_{te}	1.0	1.39	0.58
N_{tf}	1.0	1.07	0.29
N_{ce}	1.0	0.28	0.33
N_{cf}	1.0	0.82	0.32

In summary, the project successfully demonstrated the following:

- the safety performance of the prototype EPS and the ability of the system to meet all design criteria such as targets for injury prevention, engineer egress, and other functional requirements, and
- the feasibility of developing a protection system that can effectively protect engineers under moderate-to-severe collision conditions, using modern occupant protection concepts and technologies.

Based on the success of this prototype effort, we recommend further developing the design for more thorough industry demonstration. We also recommend pursuing the following suggestions as part of future research and development efforts:

- Include an abdominal injury criterion target (in addition to existing design constraints), and tailor the system to meet those requirements. It may also be worthwhile to include the tibia injury criterion;
- Verify system performance under a broader variety of test conditions (such as 50^{th} percentile female anthropomorphic test devices (ATD), offset/angled impact, etc.), first analytically, and then through physical testing, including making any revisions to the conceptual design to ensure that the protection scheme is viable over a broad spectrum;
- Optimize the system for improved performance, ergonomics, and cost efficiency,

incorporating the lessons learned and demonstrating the critical design elements and potential safety benefits;

- Study the crush/crash behavior of a modern car design under a variety of impact conditions and gather data from past impact tests to prepare detailed guidelines on trigger design based on those simulations and test results; and
- Extend the concept from cab cars to locomotives.

1. Introduction

1.1 Background

In rail vehicle collisions, the cab or locomotive engineer is frequently in a vulnerable position and at great risk of injury occupying the leading end of the vehicle. In accidents with a conventional cab car leading, the control cab often suffers the most damage because there is little energy-absorbing structure between it and the front of the car. As passenger railcars with increased crashworthiness are developed, there is significant potential for preserving the compartment occupied by the engineer. In particular, full-scale impact tests have demonstrated that the engineer's space can be preserved at closing speeds up to 30 mph [2].

When sufficient survival space is preserved, the next imperative is to protect the engineer from the forces and accelerations associated with secondary impacts. Secondary impact occurs when the rail vehicle decelerates or accelerates suddenly due to collision forces and the occupants of the rail vehicle strike some part of the interior. Given the hard surfaces and protruding knobs/controls in a cab, even a low speed collision can result in large, concentrated forces causing injuries to the engineer.

Current cab car designs have minimal interior crashworthy features. The clean cab concept of the 1970s removes sharp edges and protruding objects from the cab compartment. While this is an improvement for very low speed collisions, a more rigorous occupant protection system is necessary for higher speeds.

There is, given the availability of modern, state-of-the-art occupant protection technologies, added incentive to develop an EPS that can protect cab car engineers from secondary impact injuries in higher speed frontal collisions. Working with engineers from the Volpe Center, SA developed a conceptual design for an EPS to protect a cab engineer in a moderate-to-severe train collision (represented by the EPS test pulse, which is a 23 g, 130 ms trapezoidal crash pulse) [3], while maintaining all injury criteria within reasonable limits, without requiring input from the engineer, without restraining him or her, and without impeding egress [3, 4]. This system included a large, passenger car-style airbag with a standard inflator and a knee bolster that features off-the-shelf crushable honeycomb and deformable support brackets.

The intent of Phase II (Option A of the project) is to evaluate the actual performance of the EPS designed in Phase I by fabricating a prototype and testing it with a dynamic sled test.

1.2 Objective & Scope

The primary objective of the current phase of the development effort was to validate the performance of the EPS using a full-scale sled test. In order to meet the stated objective, the scope of the effort included the following:

a. Fabricating the baseline cab desk and the EPS components and mounting the EPS components to the baseline cab desk;

b. Outlining the test requirements and preparing the test plan for the sled test;

c. Conducting a sled test to verify EPS performance; and,

d. Comparing the test performance of the EPS with the predicted performance.

1.3 System Design Goals

The EPS was designed to do the following:

- Protect engineers from the secondary impact that occurs after a frontal train collision when the engineer strikes the control console.
- Require no action from the engineer to trigger the system.
- Allow for unencumbered exit of the engineer.
- Incorporate into the design no seatbelts or other systems that must be disengaged before the engineer can flee the cab.
- Provide compartmentalization of a 95th percentile anthropomorphic test device (ATD), and measured injury criteria for the ATD's head, chest, neck, and femur that are below the limits (see Table 2) currently specified in the Federal Motor Vehicle Safety Standards (FMVSS) 208 [5] when tested under the EPS Test Pulse (see Figure 1).

Table 2. Limiting Injury Values

Injury Criterion	Limiting Value
HIC_{15}	<700
N_{ij}	<1.0
Neck tension	<937 lbf (4,170 N)
Neck compression	<899 lbf (4,000 N)
Chest deceleration	<60 g over a 3 ms clip
Axial femur loads	<2,250 lbf (10,000 N)

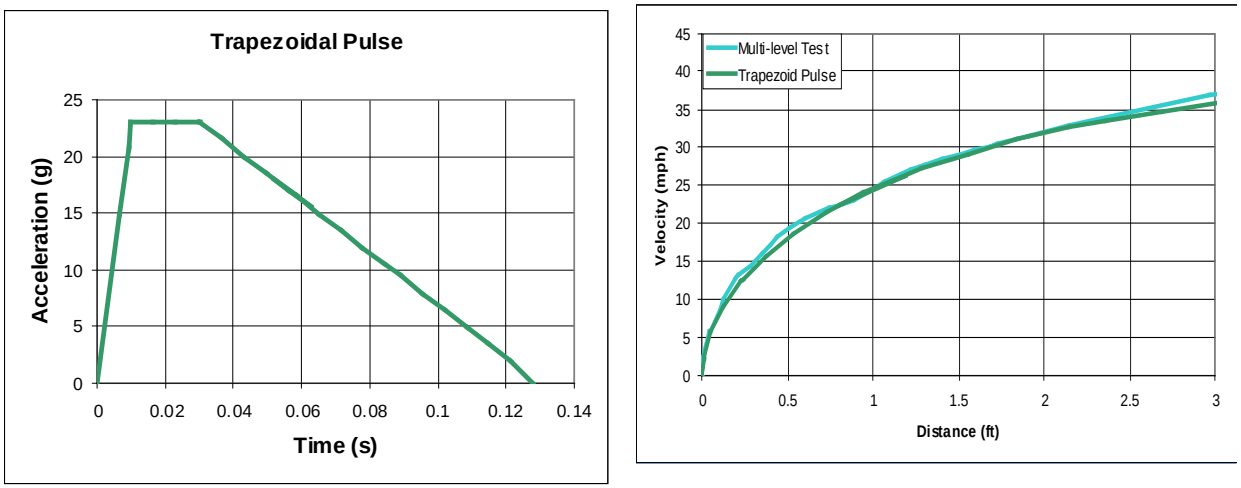

Figure 1. Crash Acceleration Pulse and Secondary Impact Velocity for EPS Test Requirements

1.4 EPS Design

The EPS consists of a baseline desk arrangement, an airbag system, and a knee bolster system (see Figure 2). The airbag system consists of an automotive passenger-style airbag installed on the top surface of the desk, an inflator, and associated electronics. The knee bolster system consists of deformable brackets and honeycomb material arranged in series along with a knee impact plate facing the engineer's knees.

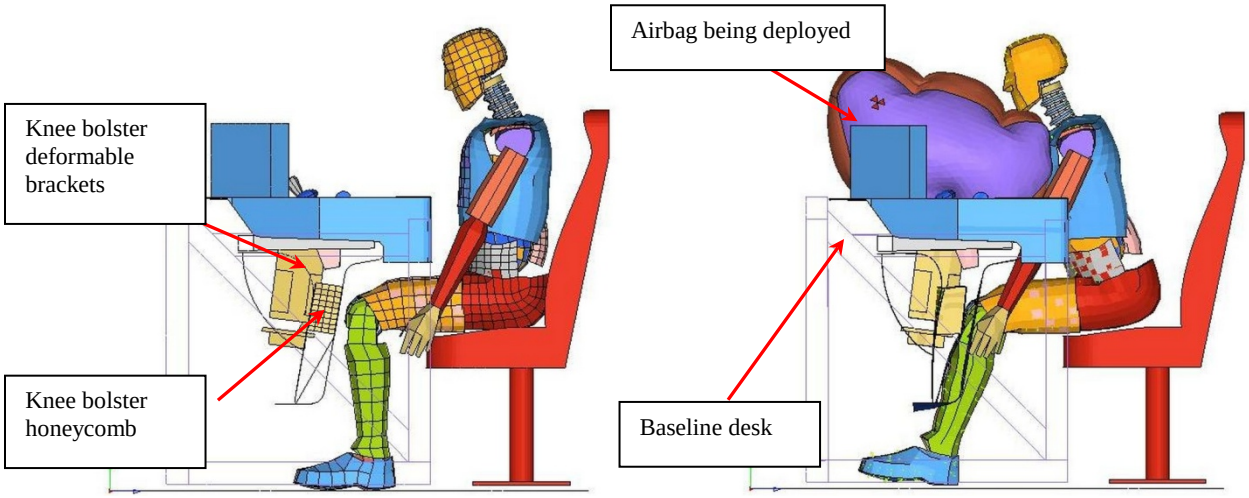

Figure 2. EPS Description

The airbag designed for this application is a slight variation on an automotive passenger side (as opposed to driver's side) airbag. A typical passenger-style airbag has a volume of 120–140 liters. The airbag designed for this project has a length of 700 mm (27.5 in), a width of 450 mm (17.7 in), and a maximum inflated volume of 155 Liters (5.5 ft^3). The airbag design can be easily manufactured using existing proven airbag manufacturing techniques. The other components of the airbag system (the control module and acceleration sensor, the trigger, and the housing for the folded airbag) are off-the-shelf items and not designed specifically for this application. The inflator is a KSS Model PH-5, dual stage, 700 KPa (101.4 psi) inflator.

1.5 System Performance

The system is designed to deploy upon impact, based on trigger signals received from car-mounted accelerometers. The two subsystems are intended to work in tandem not only to cushion the engineer, but also to control ATD kinematics. In particular, the airbag is designed to limit head, neck and chest injuries by arresting the motion of the engineer during a collision so the head, neck, and torso do not impact a very hard surface, such as the cab console. The airbag also limits the distance that the ATD has to travel before impact. In addition, the knee bolster is designed to minimize femur loads through controlled crushing of the honeycomb and brackets, while also controlling the forward movement of the ATD and reducing the tendency of the ATD to pitch forward about its abdomen.

Modeling of system performance, using a RADIOSS® [6] model with validated submodels, showed that the system would be very effective in meeting the performance goals outlined (see

Figure 3). The resulting injury indices were well below the prescribed limits, as shown in Table 3.

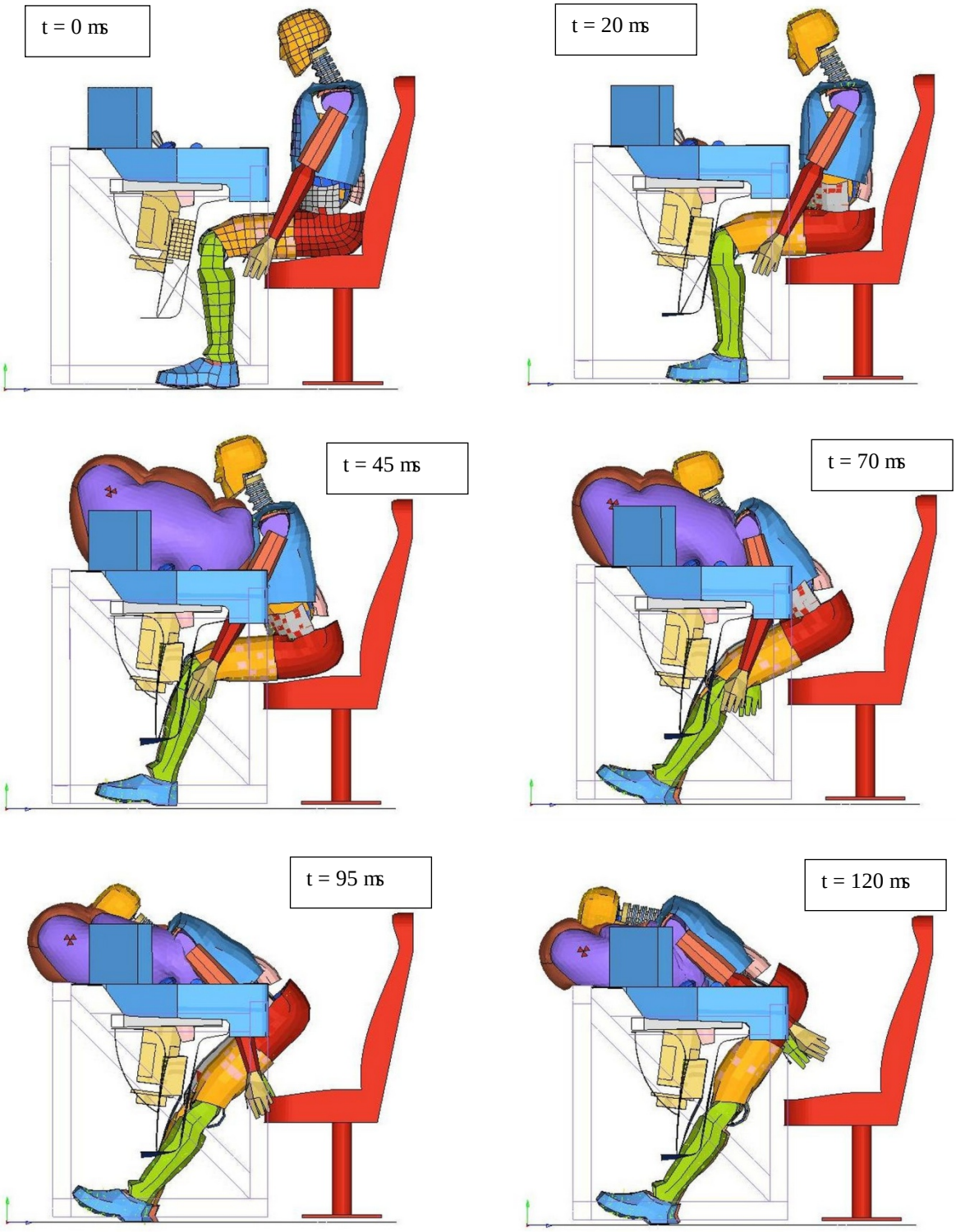

Figure 3. System Performance and ATD Kinematics for the Proposed Design

Table 3. Safety Performance of the EPS

Injury Parameter	Index Limit	Calculated Injury Indices		
		Base Case	Pre-Component Characterization Tests	Post-Component Characterization Tests
HIC_{15}	700	9,661	104	87
Chest 3 ms (G)	60	38	38	35
Femur Left (N)	10,000	20,307	7,611	7,318
Femur Right (N)	10,000	20,236	7,743	6,924
Neck Tension (N)	4,170	5,089	2,177	2,504
Neck Compression (N)	4,000	2,525	934	543
N_{te}	1.0	1.39	0.60	0.77
N_{tf}	1.0	1.07	0.25	0.29
N_{ce}	1.0	0.28	0.26	0.18
N_{cf}	1.0	0.82	0.26	0.25

1.6 Organization of the Report

This report describes Phase II (Option A) of the EPS prototype design effort: the fabrication of the prototype and results of the dynamic sled test. More specifically, Chapter 2 describes the prototype fabrication, Chapter 3 describes the test requirements and plans, Chapter 4 describes the tests and results, Chapter 5 discusses the test results in detail, particularly in comparison with the analytical models, and Chapter 6 summarizes the conclusions reached from this effort and recommendations for future work.

2. Prototype System Details and Fabrication

The prototype system that was evaluated as part of this project was comprised of three elements:

- The baseline cab desk, which simulated the dimensions of the composite cab that was designed in Phase I,
- The knee bolster system which was composed of the honeycomb structure and the deformable brackets, and
- The airbag system which was composed of the cushion/bag and the corresponding inflator.

These elements and relevant fabrication details are described in the following sections.

2.1 Baseline Cab Desk

As part of Phase I activities, the overall layout for the baseline desk was derived as a composite of several relevant engineer cabs. This layout was then extended into a detailed design, incorporating the appropriate dimensions, structural sheets and members, and connection/weld details. The design and drawing effort was completed using Pro/Engineer software. An isometric image of the baseline cab desk is presented in Figure 4.

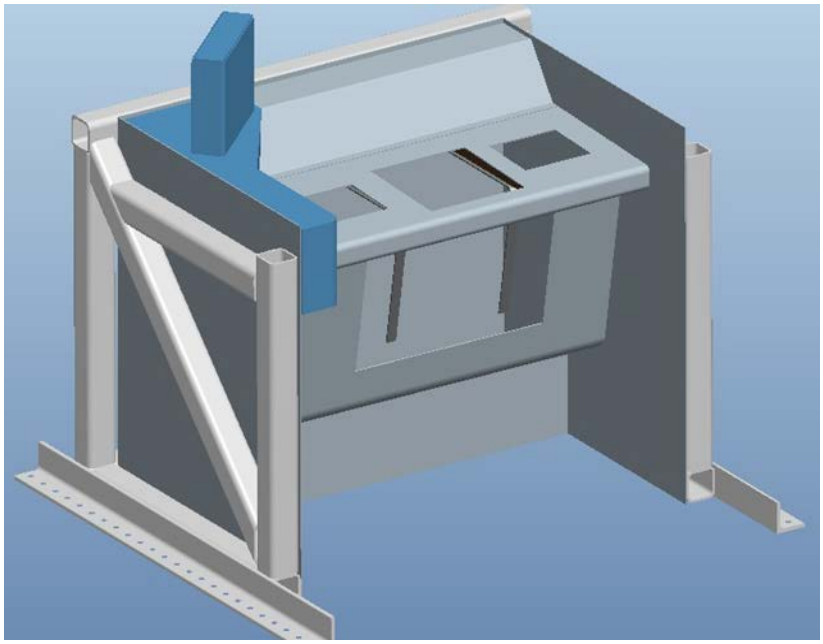

Figure 4. Model of Baseline Cab Desk (Controls Not Shown)

The baseline desk was fabricated based on the drawings created, using the appropriate materials, including steel sheets, steel tubes, etc. The desk top and side sheets were laser-cut, and then pressed into the desired shapes using appropriate machine-shop equipment. The tubes were mitered as called in the drawings. Subsequently, the structural tubes were assembled to form the skeleton, and then the sheets were welded or bolted in as appropriate. The structure was then

painted using contrasting colors for added visibility during the test. Figure 5 presents two images of the completed (pre-paint) baseline cab desk.

Figure 5. Completed Baseline Cab Desk

The seat for the test was donated by Southern California Regional Rail Authority (SCRRA), the commuter rail agency in Los Angeles, California. This was an older seat removed from one of the cab cars in the SCRRA's Metrolink service. Figure 6 presents a picture of the Metrolink seat.

Figure 6. Cab Seat donated by SCRRA

2.2 Knee Bolster System

The knee bolster system is comprised of two key elements: the honeycomb block and the deformable knee bracket. The deformable knee bracket was identical to the version that was tested during the component level tests in Phase I of the effort. The knee bolster brackets are made of ASTM A36 steel with minimum yield strength of 36 ksi, a minimum ultimate strength

of 50 ksi, and the dimensions noted in Figure 7. The deformable knee brackets were subsequently welded in to the baseline cab (Figure 7).

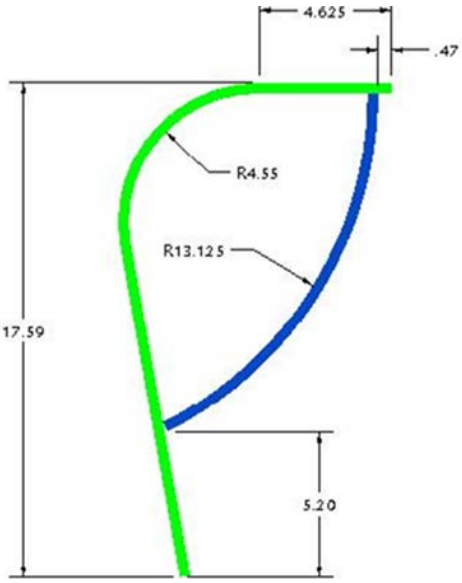

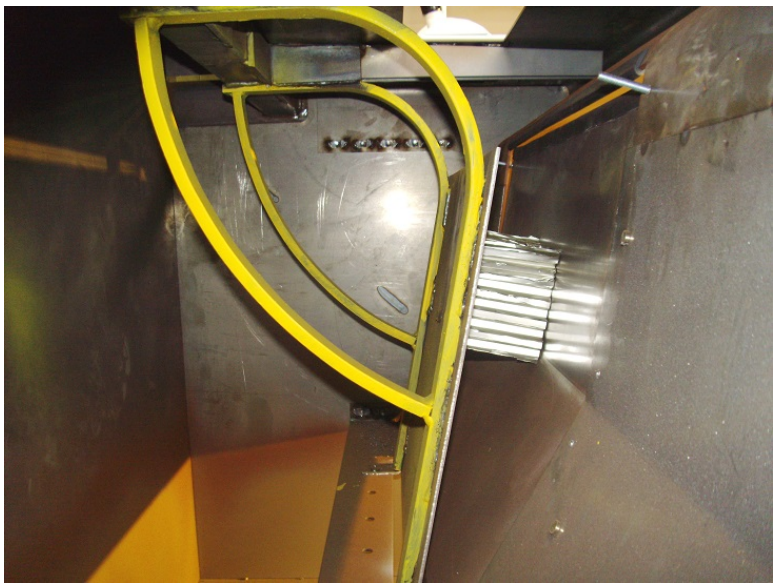

Deformable Bracket Dimensions **Installed in Desk**

Figure 7. Knee Bolster

The honeycomb material initially proposed (in Phase I) was a HexCel Corporation product HexWeb CRIII-3/8-5052-0015N-2.3. This model is made up of 3/8" hexagonal cells from 5052 aluminum with a nominal foil thickness of 0.0015" with engineered/published crush strength of 75 psi. Based on the simulation results from Phase I, it was observed that a softer honeycomb material would offer better femur protection. Therefore, a softer grade of honeycomb from HexCel with similar construction, but nominal crush strength of 40 psi was chosen for this test.

The honeycomb material was procured from HexCel in large sheets, and then cut to the right size for use within the knee bolster system. The block was fastened to the knee bolster back plate using an appropriate adhesive.

2.3 Airbag System

The airbag system is composed of an airbag and an inflator, both of which are housed in a standard automotive package. The proposed system uses a relatively large, custom design airbag that is similar to an automotive 'passenger–style' airbag, and an off-the-shelf inflator model # PH-5 from Key Safety Systems (KSS). The airbag cushion is 700 mm (27.5 in) long, 450 mm (17.7 in) wide, with a maximum inflated volume of 155 Liters (5.5 ft^3), and with two sets of internal tethers to control the desired deployed shape. The airbag dimensions and other key details of the system are presented in Figures 8 and 9.

The airbag housing is constructed of steel (stamped and plated) and houses the airbag and the inflator (see Figure 9). The housing was fastened to the top surface of the desk with the

appropriate fasteners. One of the standard airbag housings produced by KSS was slightly modified and used for this effort.

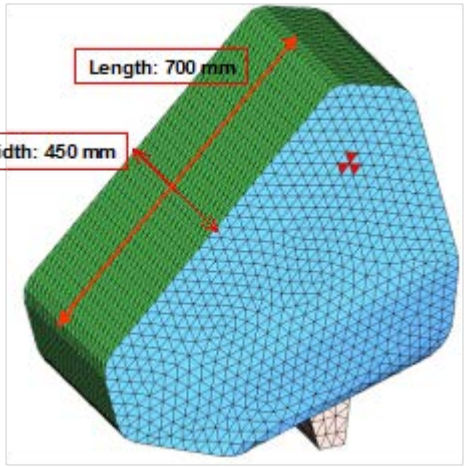

Figure 8. Airbag Shape

Airbag Configurations;

- **700mm length cushion**
- **450mm width cushion**
- **155 liters cushion volume**
- **upper / lower tether (510 / 400 mm)**
- **No vents**
- **PH-5 inflator, 700kPa (10ms time delay)**

Description Airbag Module:
• Single occupant, automotive passenger style
• Production-based design
• Module weight approx. 3.9kg

Inflator:
• Hybrid or pyrotechnic technology. 12 V connection
• Single or dual-stage inflator (700 - 500KPa)

Cushion:
• 155 liter tethered cushion. Sewn construction
• Material un-coated 630 denier PA6.6 nylon fabric

Housing:
• 1008/1010 Steel

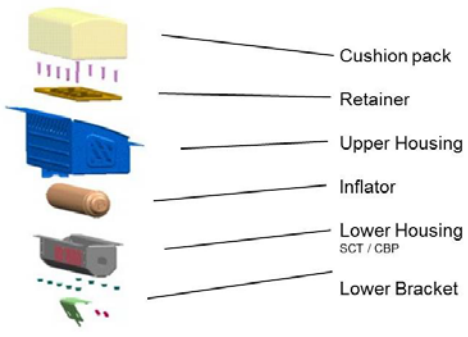

Figure 9. Airbag module details

The inflator selected (Model: PH-5) was a dual stage model with a pressure rating of 700kPa (101.4 psi), and a diameter of 45mm (1.77 inches). Figure 10 below shows a CAD image of the PH-5 inflator.

Figure 10. PH-5 Inflator

A dual stage inflator can receive two successive trigger signals to initiate full deployment/flow. In certain automotive crash conditions, such as a child being seated facing the airbag, only the first of the two stages may be triggered. Modern airbag inflators generally have two-stages as required by recent standards/regulations in the automotive industry. The two stages are usually phased 10ms apart in a deployment.

The airbags are generally triggered by an external control module. On an actual automobile (or future railcar application), the trigger module receives input from acceleration sensors, and based on the specified severity of the sensor input, triggers the deployment of the airbag. For a sled test application, the trigger module is contained in the sled test apparatus, and is triggered based on a preset time-to-fire (TTF).

The entire airbag system was fabricated and assembled by KSS at its facilities in Sterling Heights, Michigan.

2.4 Quality Control

The baseline cab, including all subcomponents and subassemblies, were fabricated and assembled using shop methodologies that are accepted in the railroad industry. SA ensured the quality of the components and assemblies, by verifying the following:

- Dimensions of the piece parts to ensure compliance with the dimensions and tolerances on the drawings
- Dimensions of the subassemblies for dimensional compliance
- Dimensions of the final desk to ensure dimensional compliance
- Verification of weld sizes at subassembly and full desk levels
- Confirmation that the right materials were used through review of material certificates
- Confirmation of honeycomb material by reviewing the thickness and cell size, as well as part number confirmation with the manufacturer

The airbag system was manufactured to KSS quality standards, which are consistent with ISO quality standards.

2.5 Assembled System

The baseline cab with the knee bolster brackets installed was shipped to the KSS test facility in Sterling Heights, Michigan upon completion of fabrication. The airbag assembly and the honeycomb block were installed into the desk assembly prior to the test. The baseline desk, ready to ship, is shown in Figure 11.

Figure 11. Completed Baseline Desk, Ready to Ship

3. Test Planning and Setup

The goal of this project was to test and validate a proposed Engineer Protection System (EPS) that is intended to protect a cab car engineer from the secondary impact that occurs following a frontal train impact, when the engineer impacts the control console. The primary objective of the sled test is to measure key parameters – including injury indices – needed to confirm that the system meets the specified performance requirements.

As part of the test planning effort, the key requirements for the system as well as the test were outlined and reviewed. The requirements were then extended into a detailed test plan for the dynamic sled test. The following sections describe the key test elements.

3.1 Test Platform

The EPS was tested using a sled based on the HYGE™ principle as shown in Figure 12. The HYGE™ principle, as described on the HYGE, Inc. webpage, simulates the longitudinal deceleration conditions of an actual impact, but in reverse. In a real-life collision event, the subject vehicle and occupant each move at the same, constant velocity, prior to impact. At impact, they are stopped very rapidly. With the HYGE™ system, the test vehicle assembly and the ATD are initially at zero velocity. This situation simulates the constant velocity conditions prior to an actual crash. The programmed rapid acceleration of the HYGE™ sled drives the vehicle assembly out from under the ATD and produces a response similar to that caused by the rapid deceleration of a moving vehicle. The acceleration and deceleration effects are interchangeable because the acceleration-time relationships are essentially the same in both cases.

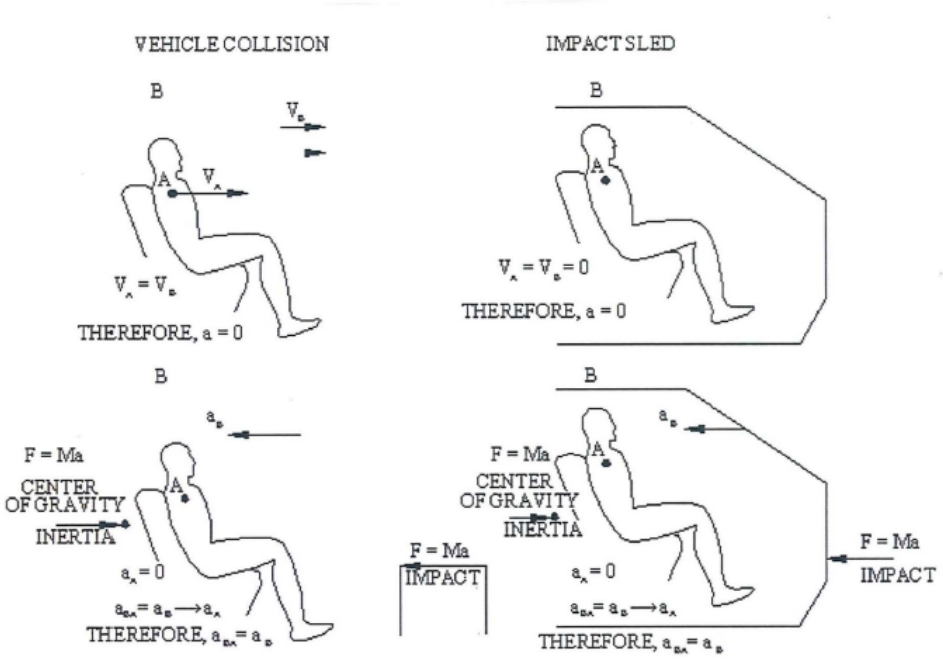

Figure 12. Sled Test using HYGE™ Principle

3.1.1 HYGE™ Operating Principle:

The HYGE™ unit develops its powerful, repeatable acceleration pulse through differential gas pressure acting on the two surfaces of a thrust piston in a closed cylinder (see Figure 13). The cylinder is separated into two chambers by an orifice plate. The area of one entire piston face is subjected to the gas pressure in chamber A. On the other side of the piston, only the smaller area within the seal is exposed through the orifice opening to the gas pressure in chamber B.

In preparation for the firing, compressed gas is introduced into chamber B until the forces on the thrust piston are equalized. Any further increase in the pressure in Chamber B upsets this equilibrium, opens the seal at the orifice, moves the piston away from the orifice plate, and instantly exposes the entire piston area (in the absence of a metering pin) to the gas pressure in chamber B, resulting in a controlled thrust on the piston. Transmitted by the thrust column, this limited duration thrust acts upon a test specimen to produce predictable acceleration.

The thrust and mass of the specimen govern the acceleration of the specimen. To produce a given acceleration waveform, a specific metering pin is attached to the thrust piston and projects through the orifice into chamber B. The contour of the pin meters the flow of gas through the orifice, regulating the acceleration and making the utilized thrust precisely repeatable.

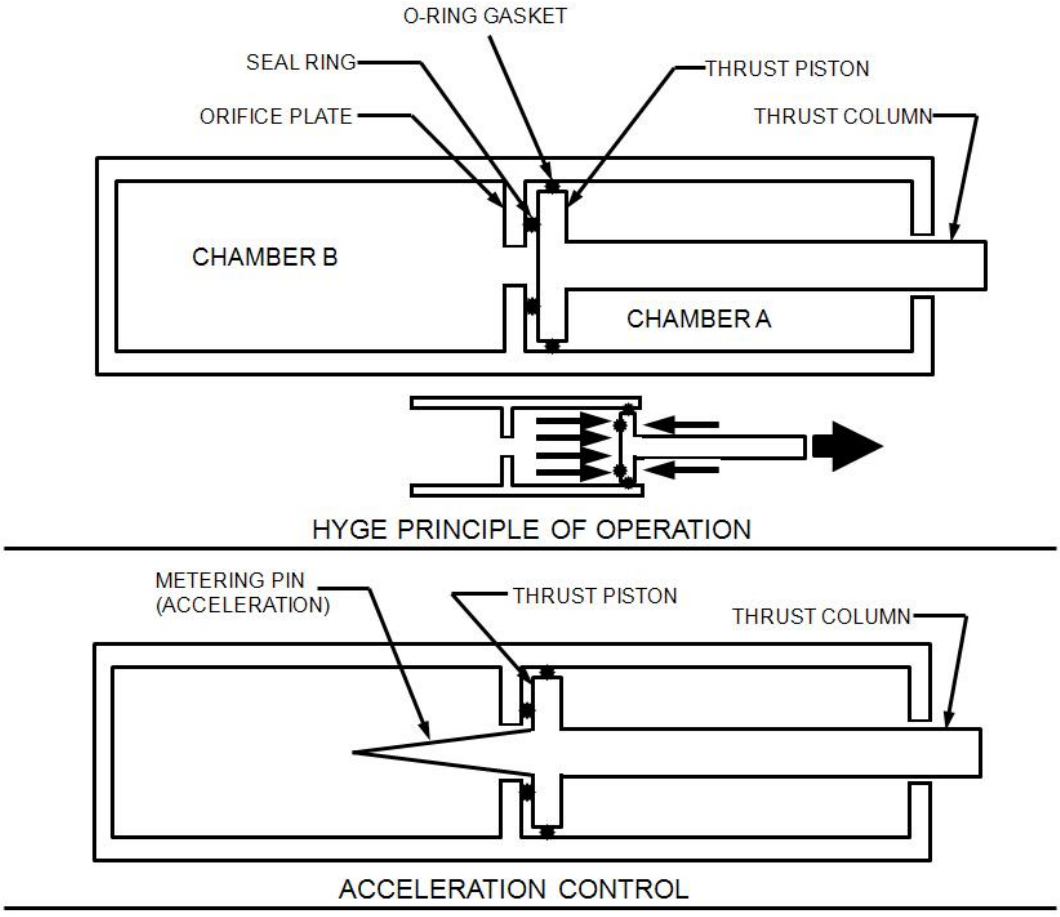

Figure 13. Schematic of HYGE™ Thrust Cylinder Operation

For this effort, a specific metering pin profile was developed and used to generate a crash pulse that closely matched the target trapezoidal EPS pulse. The test pulse was compared to the target pulse as per the methodology outlined in SAE standard, AS8049 Appendix A, and confirmed to be a valid representation of the target pulse (see Figure 14). Figure 14 further compares the secondary impact velocities from the test and target curves to highlight the similarities. A picture of the metering pin that resulted in the test curve is shown in Figure 15.

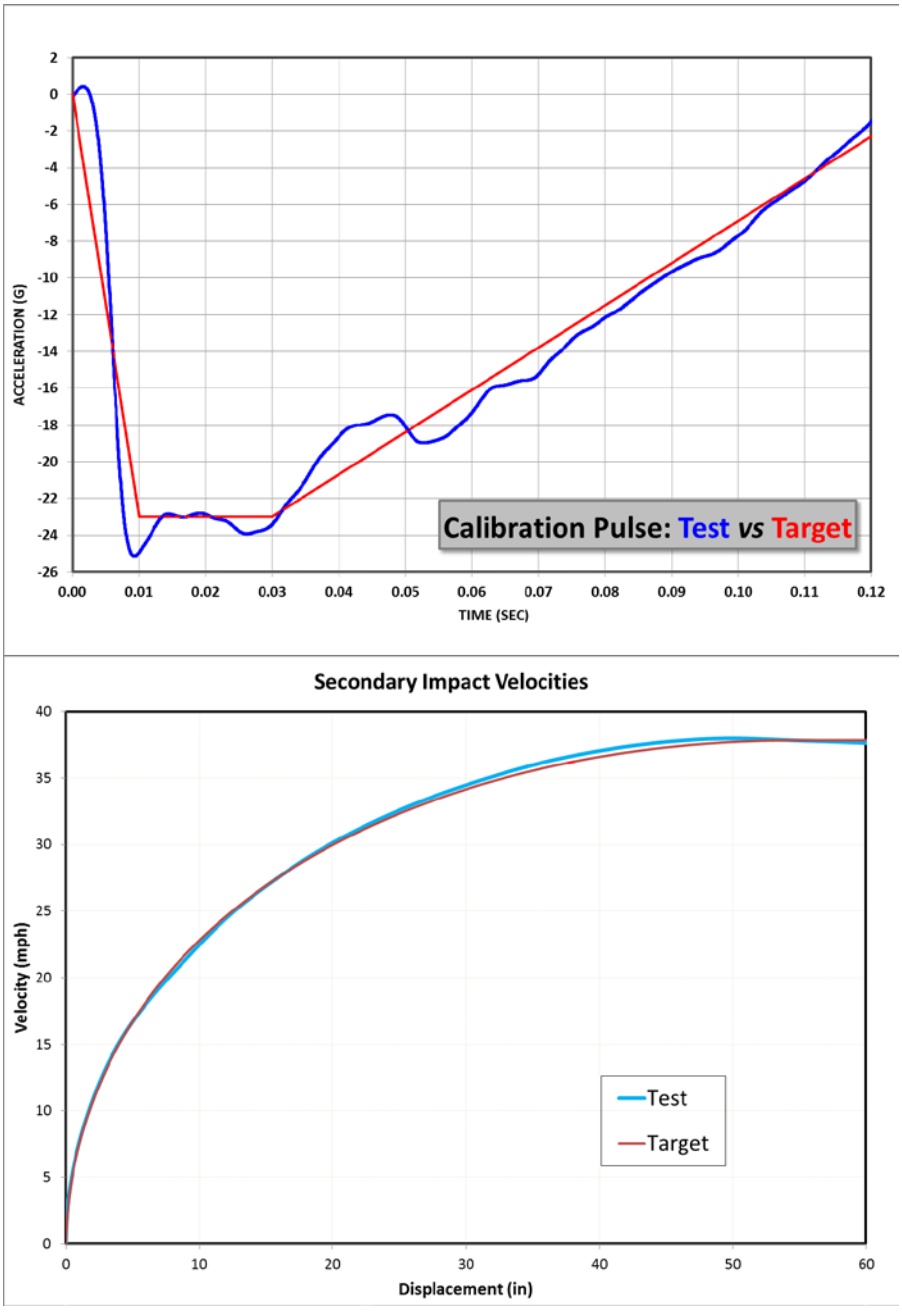

Figure 14. Comparison of Test and Target Pulses

Figure 15. Metering Pin Profile

The key advantages of the application of the HYGE^{TM} principle to crash simulation testing are:

- The ATD can be accurately positioned prior to the test and the position will remain unchanged until the instant of impact.
- Prior to impact, the ATD and the seat assembly are not subjected to forces caused by compressed seat springs or energy stored in the ATD.
- The zero acceleration level of the ATD prior to impact closely simulates real constant velocity conditions.

3.2 Test Article Description

The sled platform contained the following items:

- The EPS (baseline desk arrangement, airbag system, and knee bolster system),
- A 95th percentile male, Hybrid-III ATD, in accordance with 49 CFR Part 572, Subparts B & E, positioned in accordance with SAE AS8049 [7],
- An engineer's seat, and
- Required instrumentation, data acquisition system, and high speed video cameras.

3.3 Test Setup and Key Parameters

The sled test was setup as follows:

- The EPS, the seat and the ATD were installed on the sled test base plate.
- The EPS and the seat were securely mounted to the test base plate to ensure that the acceleration pulse was positively transmitted to those structures.
- Seat assembly was reinforced to ensure structural integrity during the test. There was a concern that the seat attachment strength would not be adequate for the test conditions.
- The ATD was positioned on the seat to simulate the forward-facing position of a cab engineer and aligned with center line of the airbag.

- The ATD was unbelted but tethered, such that the tethering did not influence the ATD impact with the EPS.
- The hands of the ATD were positioned hanging to the sides to match the FE model.
- Floor-to-desk top and seating heights approximated the FE model (Table 4 and Figure 16).
- The face, hands, and knees of the ATD were chalked with varying colors to capture the ATD surface in contact with the airbag.
- The airbag trigger mechanism was setup to trigger 12ms after the crash pulse initiation, with the secondary inflation occurring a further 10ms later.

Table 4. Test Setup Parameters

Parameter	**Value**
H-Point, or Hip-point (vertical, from floor)	24.48”
Knee Center Point (vertical, from floor)	21.45” – 22.05”
Gap between Knee & Front Bolster plate (longitudinal)	1.18”
Top Edge of Desk (vertical, from floor)	30.9”
Knee center-to-center (lateral)	8.62”

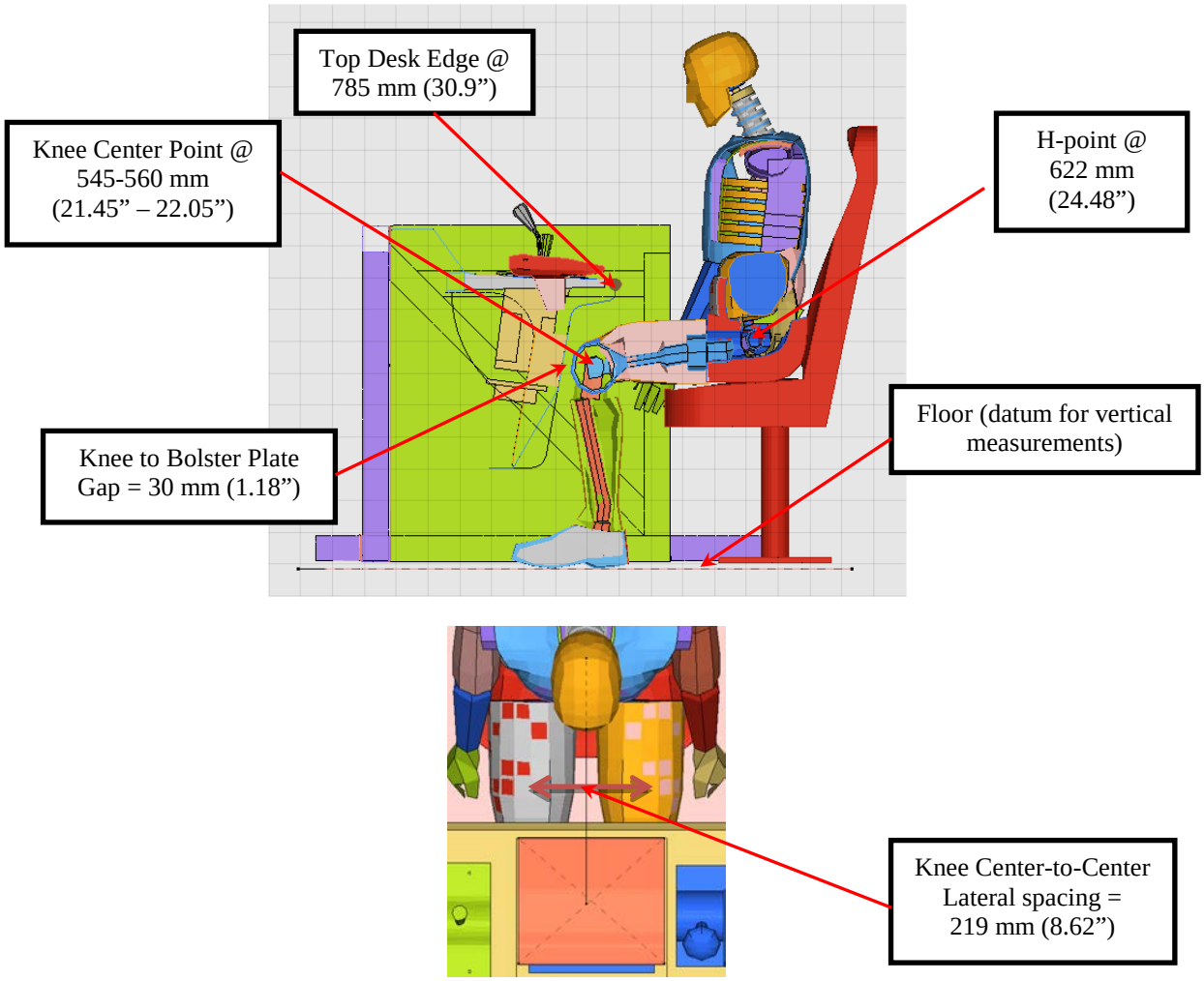

Figure 16. ATD Positioning Parameters from Finite Element Model

3.4 Instrumentation and Data Acquisition

Instrumentation and data acquisition were applied as follows:

- Acceleration of the sled base plate
  - Two (2) tri-axial accelerometers were applied to the EPS, one approximately at the center of the baseline cab desk and the other near the seat adapter plate.
- A 95th percentile male, Hybrid-III ATD, in accordance with 49 CFR Part 572, Subparts B & E, was positioned in accordance with SAE AS8049. ATD positioning was confirmed using a coordinate measurement frame, with a laser pointer that focused on key ATD points. The ATD was instrumented to measure the time history of the following parameters:

- Triaxial head acceleration
- Triaxial chest acceleration
- Uniaxial chest deflection
- Triaxial upper neck force
- Triaxial upper neck moment
- Axial femur load (left and right)

- Sled acceleration and ATD sensor data were acquired using a Data Acquisition System (DAS), which is based on the Kayser-Threde (K-T) MiniDAU.
  - Each unit was physically attached to the sled carriage. The units are therefore highly ruggedized and have been designed to withstand repeated acceleration shocks of very high magnitude.
  - The DAS provided the needed excitation voltage, analog-to-digital conversion (ADC), and the signal conditioning needed for each channel. Accuracy is specified as 0.2%.
  - Antialiasing was accomplished via 4 kHz, 6-pole Butterworth low-pass filters. Separate 12-bit ADCs are used for each channel, with peak throughput of 20 kHz. Flash memory was used to store collected data, so no battery is needed to preserve the memory contents.
  - Post-processing was consistent with the provisions in SAE J211-1 and SAE J1733.
- The dual stage airbag was triggered on a time basis using a sled mounted electronic module with a Time-To-Fire (TTF) of 12 ms for the first trigger, and 22 ms for the second trigger (10 ms gap between the triggers). TTF is measured from the zero-time point on the idealized test pulse.
- Data were collected at 20,000 samples per second.
- All data were filtered using the appropriate filters (channel classes) defined in SAE J211 for the particular injury index. The following injury criteria were computed in accordance with 49 CFR571.208 and SAE J211.1:
  - HIC_{15}
  - Chest acceleration (3ms clip)
  - N_{ij} (i.e., N_{te}, N_{tf}, N_{ce}, N_{cf})
  - Peak upper neck axial tension and compression forces
  - Peak axial femur load
  - Peak upper neck extension/flexion moment
- High Speed Video
  - Four (4) high-speed video cameras were used as follows:
    - One overall right side view of the setup

        - One close-up side view to capture knee bolster crush
        - One close-up side view to capture ATD knee movement
        - One low, angular view from rear to capture knee to knee bolster gap closure.
    - The cameras were setup to capture video at the rate of 1,000 frames per second.
    - Multiple crosshair targets were placed on the ATD, the seat, and the desk to permit effective post-test analysis.
    - Sufficient lighting for high quality photometric analysis of the video was arranged.
- Deformation measurements
    - Relative location and shape of the knee bolster deformable brackets were measured before and after the test to determine amount of total permanent set on the bracket geometry.
    - The crush-time history of the honeycomb material was developed from a photometric analysis of the high-speed video.
    - Amount of permanent crush in the honeycomb material was measured post-test.
- Still Images
    - A digital camera was used to take still photographs of the sled, the test setup, the baseline console, airbag, knee bolster, ATD, and seat, pre- and post-test.

3.5 Summary of Test Setup

This chapter described the various elements of the test setup, including the test articles, ATD setup, instrumentation, and data acquisition, along with a brief description of the principles behind sled testing. The next chapter describes the test process and results.

4. Test Effort and Results

The first sled test was conducted in the laboratory at the KSS headquarters in Sterling Heights, Michigan, on October 26, 2012. The test article and instrumentation were prepared as outlined in the previous chapter. Figure 17 presents four views of the initial test setup, with the ATD in position, and all instrumentation and video cameras mounted.

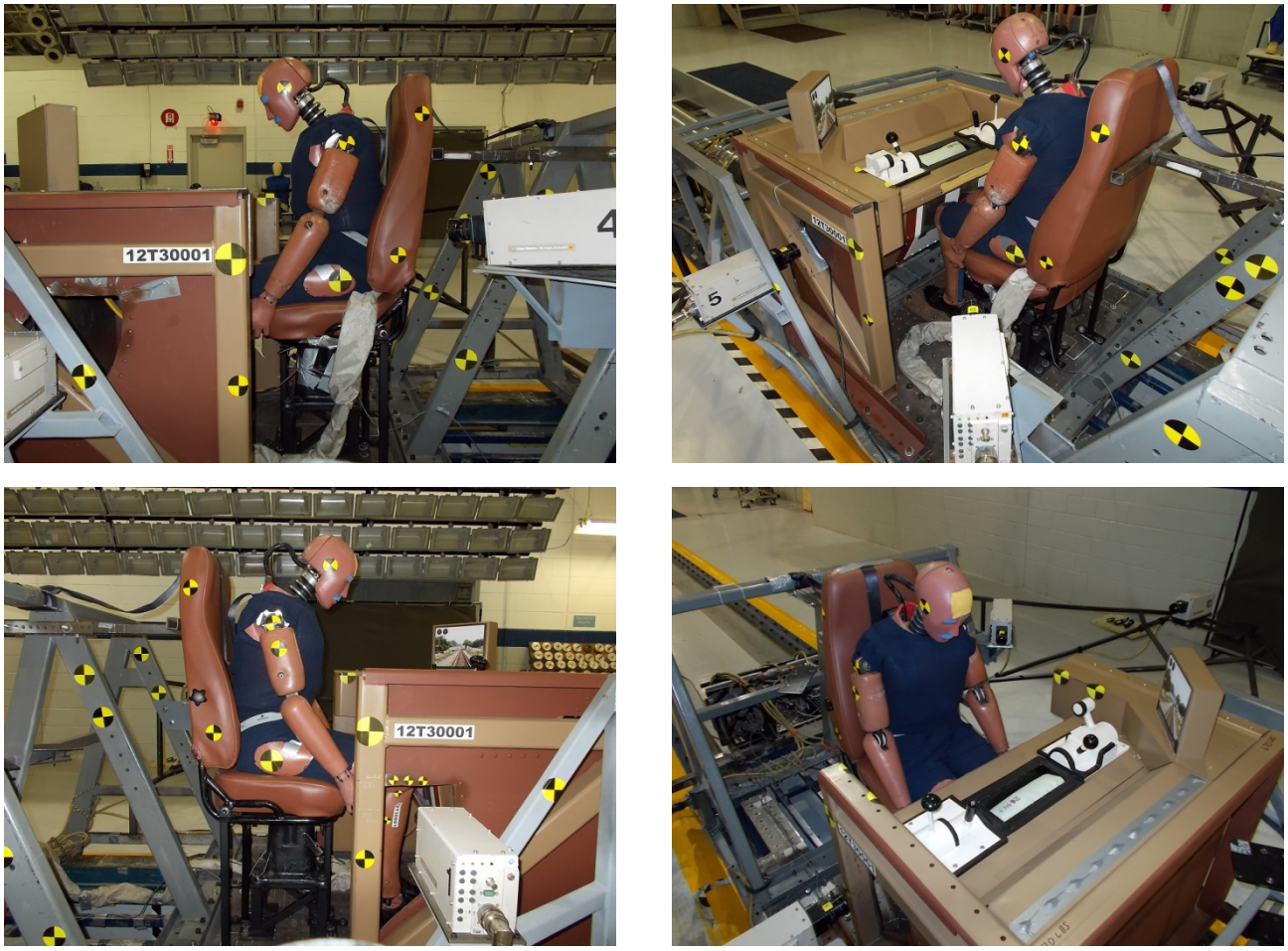

Figure 17. Sled Test Setup (Initial Test) – Ready for Test

4.1 Test Process

The test sequence was as follows:

- Data acquisition system and high speed video capture were initialized.
- A 23G test acceleration pulse, as shown in Figure 14, was applied to the sled.
- The airbag was triggered (automatically) 12ms after crash pulse initiation.
- A mechanical brake system acting between the sled and the sled rail decelerated the sled to a stop following the pulse. This brake is on all the time, but the thrust from the HYGE™ cylinder is compensated to produce the desired acceleration profile, considering this additional loss.

- Post-crash, the condition of the honeycomb, deformable brackets, the airbag and the ATD were inspected.
- Collected data were saved and processed.

4.2 Initial Test Results

As noted earlier, the honeycomb used for this effort was changed from the specification called out in Phase I, in expectation of improved performance. Phase I simulations (see figure 3) showed a 'less than ideal' level of honeycomb crush. For the current effort, the crush strength of the honeycomb was dropped from 75 psi to 40 psi. A new set of RADIOSS® simulations with the revised honeycomb properties was run, resulting in moderate improvements in injury indices for the knees, without any notable negative effect on the other indices. Table 5 presents the results of these updated, pre-test simulations, along with the observed test results.

Table 5. Injury Indices—Comparing Pre-test Predictions to Results from Test 1

Injury Parameter	Index Limit	Injury Indices	
		Pre-test Predictions	Sled Test 1
HIC_{15}	700	91	143
Chest 3ms (g)	60	32	28
Femur Left (N)	10,000	6,506	6,227
Femur Right (N)	10,000	6,594	7,952
Neck Tension (N)	4,170	2,237	2,178
Neck Compression (N)	4,000	1,245	3,412
N_{te}	1.0	0.68	1.60
N_{tf}	1.0	0.12	0.50
N_{ce}	1.0	0.19	1.10
N_{cf}	1.0	0.25	0.19

As seen in the table above, two of the neck injury indices, N_{te} and N_{ce}, which are measures of neck extension were above the targeted limits for the test. Review of the ATD kinematics from the test, presented in Figure 18, highlights the issue. It is seen that the airbag deploys in a trajectory that initially contacts the face/chin area, thereby loading the neck in extension. It was also seen that in the initial ATD positioning, the neck was leaning forward more than usual, contributing to the high injury values, though in real life, this condition may not always be avoidable.

Under ideal deployment conditions, an airbag would not interact with the ATD until it is almost fully deployed. In automobiles, this can be achieved by the effective use of seatbelts; but in cab cars, given the present need to avoid restraints, this must be achieved by geometric and bag design efforts. In this case, it was seen that the airbag was interacting with the ATD during the deployment phase. This concern is further complicated by the fact that, while the usual airbag modeling techniques used in the automotive industry do represent the fully deployed performance of the bag well, they capture the deployment sequence itself with less fidelity.

Figure 18. ATD Kinematics from Sled Test - 1

4.3 Alternate Configuration Studies

The design team reviewed several options for solutions to the problems observed above, including:

- Locating the airbag further forward (away from the occupant) on the desk
- Tilting the airbag mounting through a housing change to permit the airbag to deploy more vertically
- Effecting a change to the deployment sequence by changing the initial fold pattern of the airbag
- Altering the internal airbag tether lengths to better control airbag shape
- Adding vents to soften the initial contact
- Altering the deployment time (TTF) by either changing the time delay for the initial trigger (12 ms) or the secondary trigger (an additional 10 ms)

Based on the technical review, it was determined that the best course of action was to effect change through airbag fold and potential tether length changes, with airbag tilt being a secondary option. The option for altering deployment time was not pursued for two reasons: first, the initial trigger delay of 12 ms is fairly short, and in real life conditions would be needed to effectively detect a collision event and take action. Second, the initial trigger is responsible for over 80% of the inflator flow, making any reductions to the delay between the first and second triggers only mildly effective, at best. The option of adding vents was not pursued due to the potential for a late head strike against the console, if the bag vented too quickly.

Several airbag fold pattern, tilt, and tether options were studied using a series of static deployment tests. The various design iterations included:

- Tilting the airbag mounting by 25 degrees (maintaining the original fold design, of a forward roll)
- Reverse double roll configuration
- Reverse single roll configuration
- Reverse single roll configuration, with reduced tether lengths (the tether close to the occupant reduced by 6" and the tether away from the occupant reduced by 3")

Static deployment tests were conducted with the airbags mounted on the desk, with no external energy/force applied to the bag (i.e., there was no movement of the sled), with the ATD positioned as it was positioned during the sled test (for reference only). The process of inflation, time of inflation, etc. were monitored with high speed video cameras to capture the air bag's deployed shape and sequence. The test results were reviewed with primary focus on the space between the ATD and the airbag prior to full deployment (about 45 ms), with particular attention paid to the possibility of loading the head and neck. The level of abdominal protection offered was also given secondary consideration.

Based on this review, the reverse single roll configuration with shortened tethers was chosen for a subsequent sled test. Figure 19 outlines the deployment sequence observed in the static

deployment test for this configuration. Appendix A presents results of all the static deployment tests completed.

Figure 19. Airbag Deployment Sequence – Reverse Single Roll with Shortened Tethers

4.4 Second Sled Test and Results

The second test was conducted on February 26, 2013. The test articles were prepared as outlined earlier. For the airbag, the "reverse single roll with shortened tethers" configuration was implemented. The knee bolster (honeycomb and brackets) that was deformed during the first test was cut out, and new brackets and a new honeycomb block were installed. The ATD was positioned similarly, except that the neck and head were positioned in the originally intended position, rather than the slouched position used in the first test. However, it was fully expected that the EPS would protect the engineer in the slouched position as well, based on the deployment sequence of the revised airbag. Figure 20 presents two images from the setup for the second test.

Figure 20. Sled Test Setup—Second Test

The measured injury indices from the second test are outlined below (Table 6), with the ATD kinematics outlined in Figure 21. As shown, the EPS was effective in protecting the engineer and keeping all injury indices within limits, while also maintaining effective compartmentalization. The next chapter presents the results in more detail, along with comparisons against the predicted measurements.

Table 6. Measured Injury Indices—Second Test

Injury Parameter	Index Limit	Injury Indices	
		Pre-test predictions	Sled Test – 2
HIC_{15}	700	91	144
Chest 3ms (g)	60	32	32
Femur Left (N)	10,000	6,506	8,426
Femur Right (N)	10,000	6,594	8,996
Neck Tension (N)	4,170	2,237	1,951
Neck Compression (N)	4,000	1,245	1,200
N_{te}	1.0	0.68	0.58
N_{tf}	1.0	0.12	0.29
N_{ce}	1.0	0.19	0.33
N_{cf}	1.0	0.25	0.32

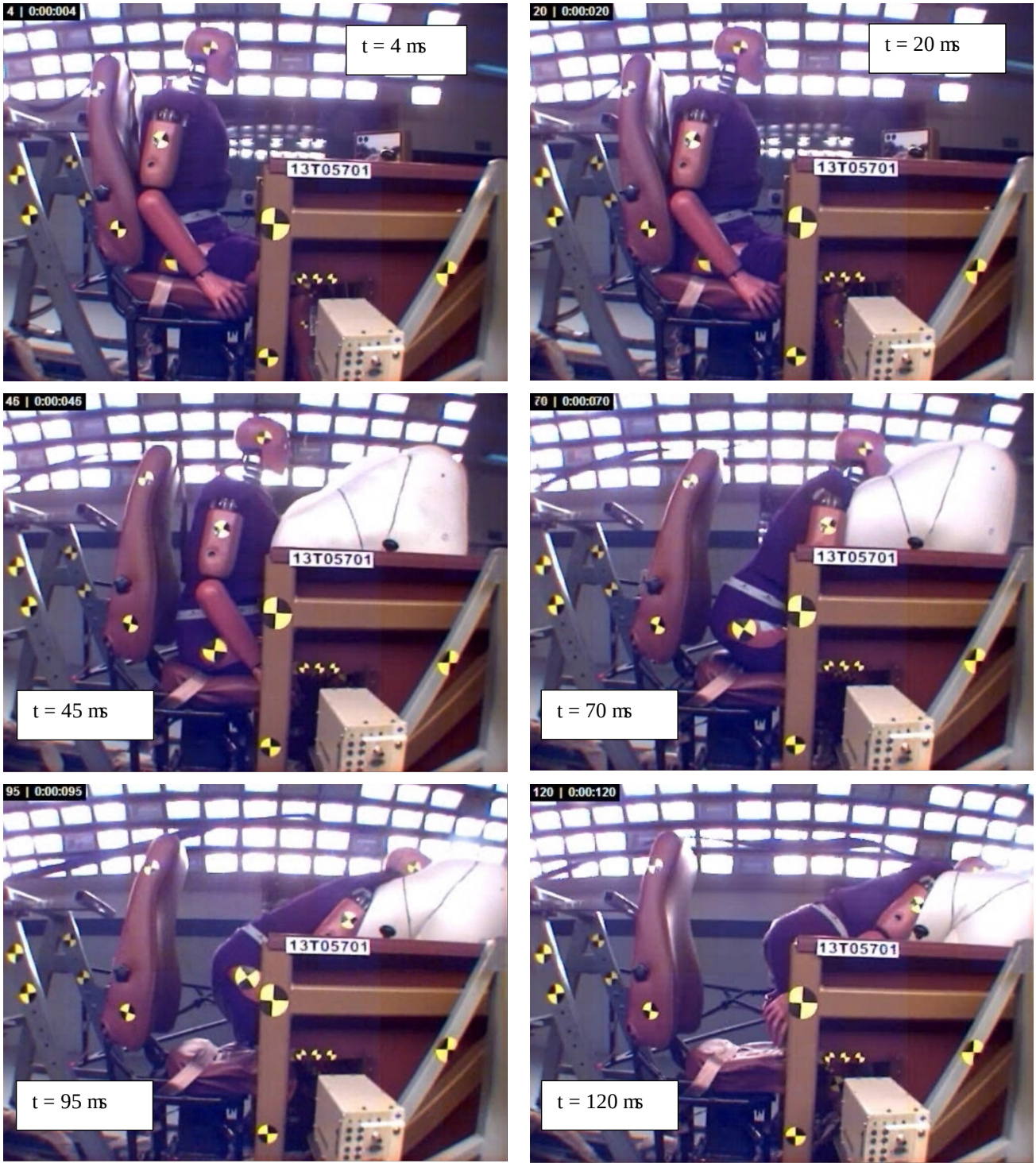

Figure 21. ATD Kinematics from Sled Test—2

5. Discussion of Test Results

Results from the second test were reviewed, not only to evaluate the performance of the system, but also to compare with the pre-test predictions. Given the potential for statistical variances in system behavior, even between two nominally 'identical' scenarios or designs, the test results compared to the pre-test predictions reasonably well, not only in peak magnitudes, but also in overall behavior. Nonetheless, a few model updates were made, with limited success, with the intent of improving correlation between the model and test. The following changes were made to the pre-test model:

- Airbag tethers were shortened to reflect the tether changes,
- Airbag mass flow was reduced by 5 percent,
- Knee bolster brackets were thickened by 31 percent, and
- Knee bolster honeycomb strength was increased by 27 percent.

As seen in Table 7, the changes improved the femur injury correlations, but did not help the head and chest injury correlations. The following sections compare and contrast the test results to both the pre-test and post-test model results and discuss the reasoning behind the changes attempted.

Table 7. Comparison of Injury Indices

Injury Parameter	Index Limit	Injury Indices		
		Pre-test Model	Sled Test – 2	Post-test Model
HIC_{15}	700	91	144	88
Chest 3ms (G)	60	32	32	35
Femur Left (N)	10,000	6,506	8,426	8,148
Femur Right (N)	10,000	6,594	8,996	7,073
Neck Tension (N)	4,170	2,237	1,951	2,211
Neck Compression (N)	4,000	1,245	1,200	970
N_{te}	1.0	0.68	0.58	0.76
N_{tf}	1.0	0.12	0.29	0.35
N_{ce}	1.0	0.19	0.33	0.18
N_{cf}	1.0	0.25	0.32	0.19

5.1 ATD Kinematics

One key observation from the ATD kinematics of Test 2 compared with that of Test 1 is that in Test 2 interaction between the ATD and the airbag is minimal until the airbag is almost fully inflated (Figure 22 highlights the difference.). This desirable outcome was one of the key goals of the static deployment tests that were conducted. Future development efforts should keep this as a key design goal for optimum safety performance. Another related observation is that, given the space between the ATD head and the airbag early in the deployment, even under slouched ATD conditions, interaction between the airbag and ATD head would have been minimal,

thereby avoiding the spike in neck forces/moment that caused concern in Test 1. The model should be capable of confirming this assumption, but the analysis was not performed.

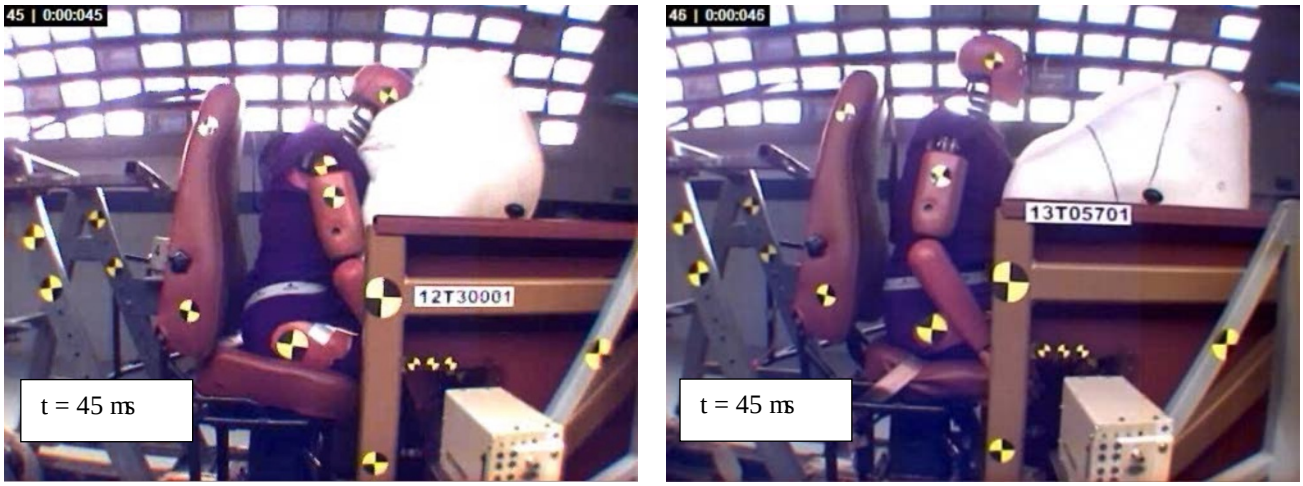

Test 1 **Test 2**

Figure 22. Comparison of ATD-Airbag Interaction Prior to Full Airbag Deployment

Figures 23a and 23b compare the ATD kinematics from the test and modeling efforts. It is clear from the images that the kinematics are very similar across all three; some minor differences observed include:

- Minor differences in the shape of the airbag, which result in slightly different initial contact between the head and the airbag; and
- The test airbag seems to slide off the front end of the desk a little more than the model airbags, especially later in the event (after 100 ms). Consequently, the test ATD leans over a bit more than the model ATD.

A review (from another camera) of the movement of the knees also showed very similar kinematics between the simulations and the test.

5.2 Head Accelerations

Figure 24 compares the head acceleration and HIC_{15} indices for the three cases. While the kinematics were very similar, a few differences were evident from this review.

The pre-test simulation results indicated a spike around 55 ms; to address this, the airbag flow rate was reduced slightly to see if that would have any effect on the spike. This reduced airbag flow rate could ideally also compensate for the constrained airbag volume with the shorter tethers. As seen in the post-test simulations, this reduction did not make much of a difference to that initial spike. Since the peak HIC values occur later in the sequence (and not at the spikes), there is no significant concern about the spikes from an overall correlation standpoint.

The post ~80 ms simulation curves (the period during which the ATD is compressing the airbag) underestimate the results obtained from the physical test, but are of a similar overall duration. Overall, the HIC numbers are comparable between test and simulations and are also substantially

below the FMVSS target limits, giving us confidence in using the model results for design.

Test	Pre-Test	Post-Test	
	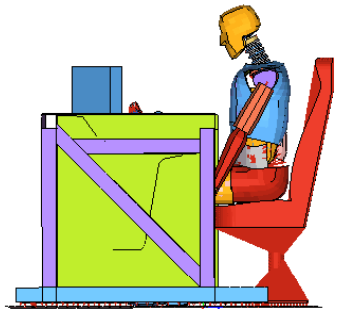	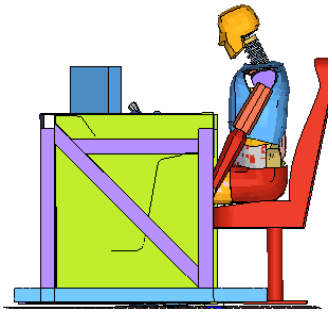	20 ms
	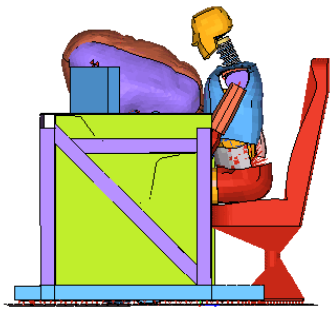	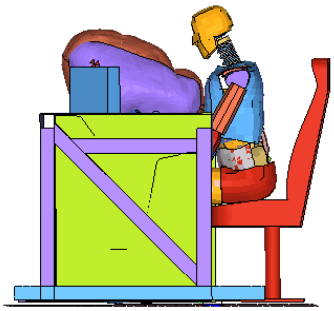	40 ms
	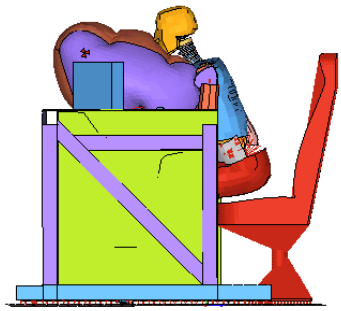	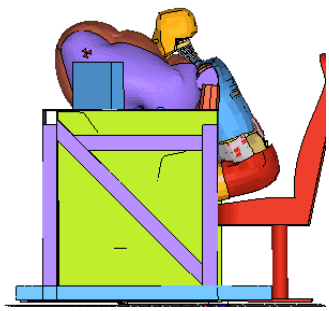	60 ms
	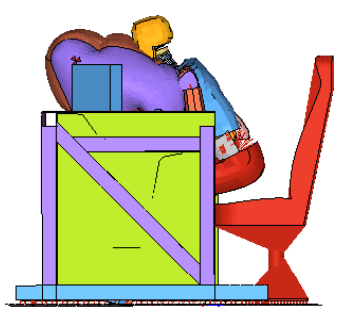	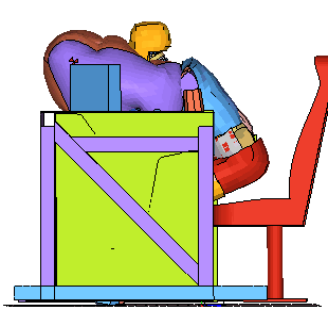	70 ms
	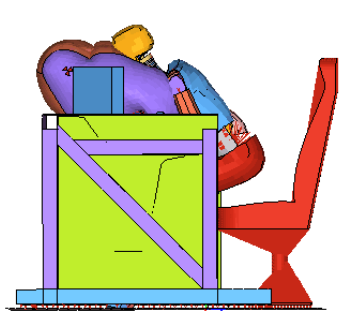	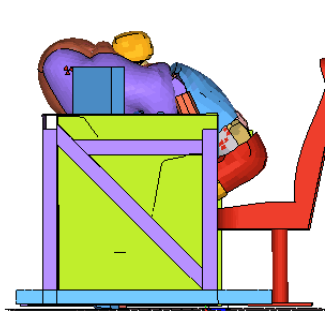	80 ms

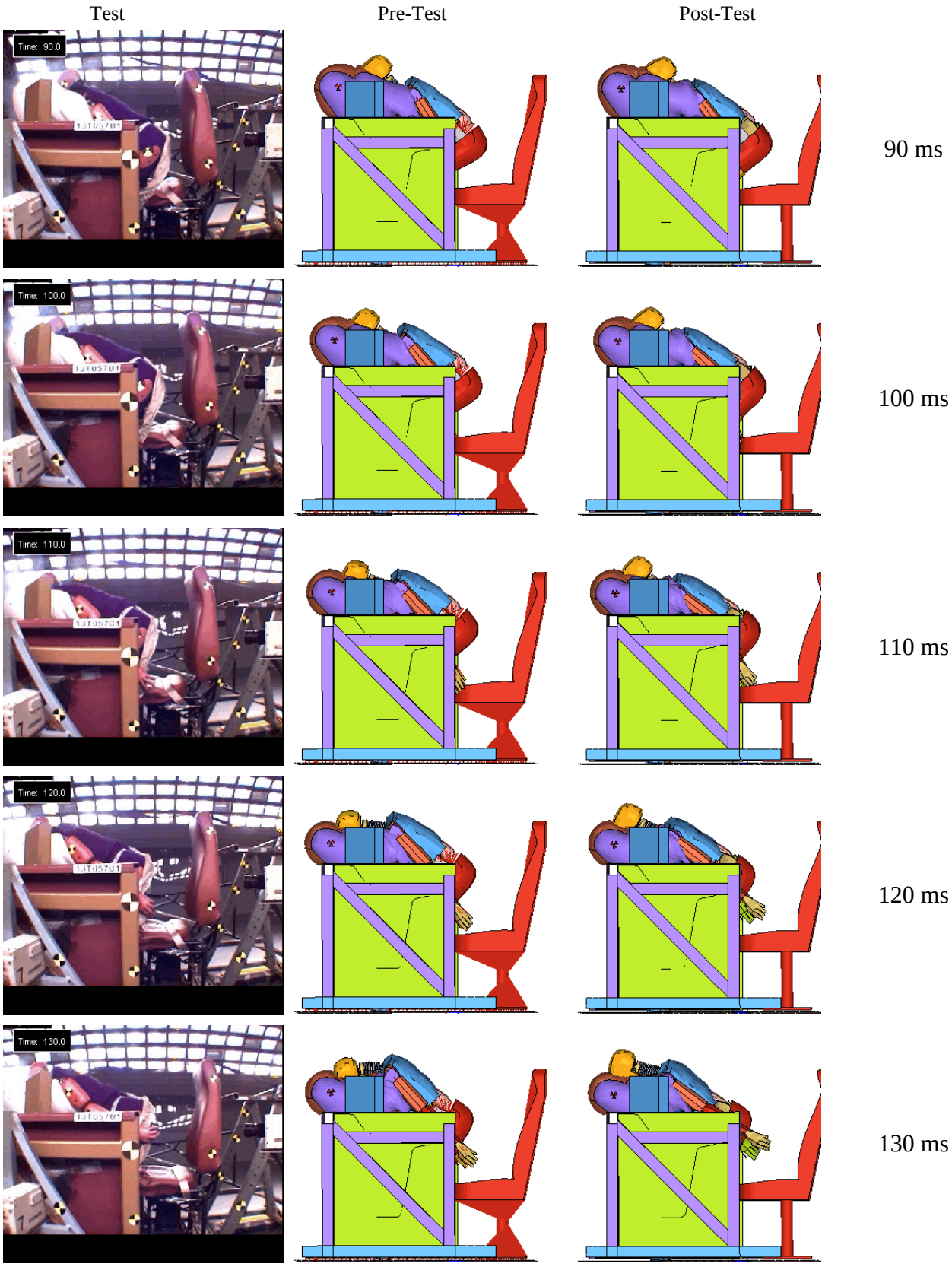

Figure 23. Comparison of Model to Test—ATD Kinematics (20–130 ms)

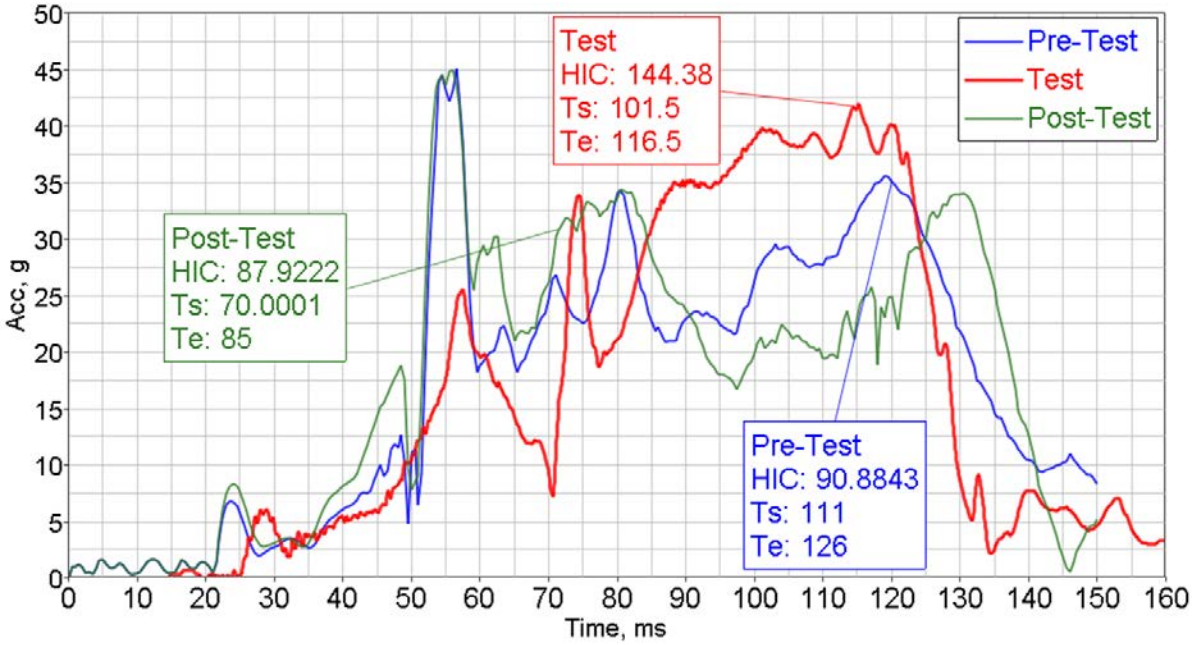

Figure 24. Comparison of Head Accelerations and HIC_{15} indices

5.3 Chest Accelerations

Figure 25 compares the chest accelerations. While the peak acceleration numbers are very similar, some variations in timing are evident. In the simulations, it appears that the chest accelerations peak sooner in the model than in the test. In the test, the initial contact is gentler than in the model, and builds up more towards the end of the run. This might again point to the airbag sliding (longitudinally) more in the test than it does in the simulation. Any concerns about these differences are somewhat allayed by the fact that the measured indices are well below the limits.

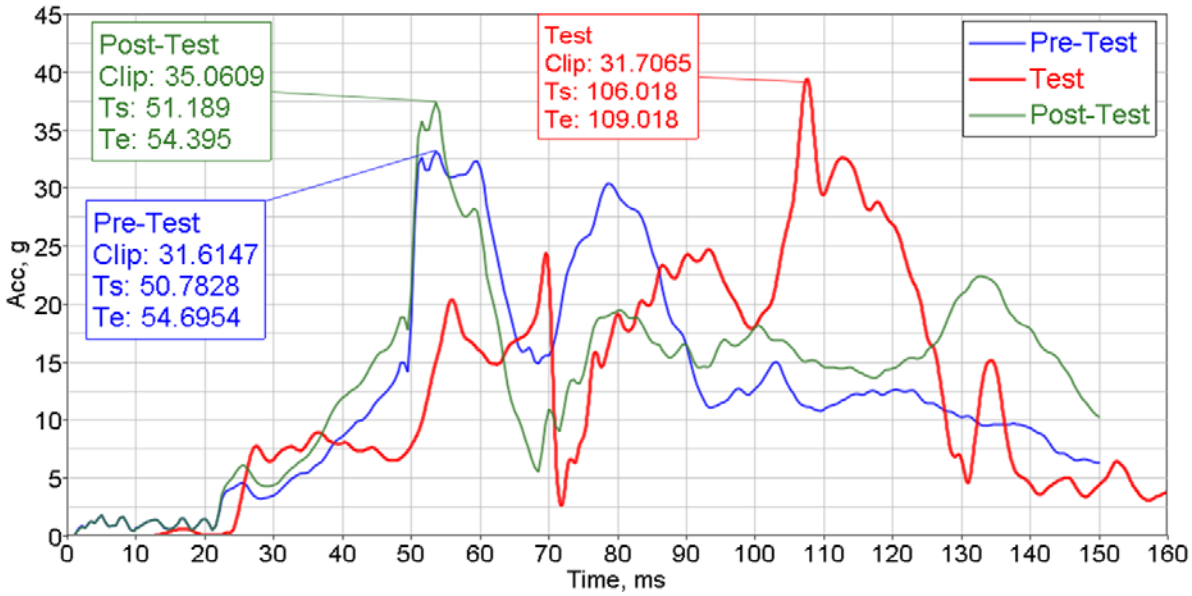

Figure 25. Comparison of Chest Accelerations

5.4 Femur Loads

Femur loads from Test 1 compared reasonably well with the predicted values; however, the loads were higher (and the bracket deflection lower) for Test 2, indicating a stiffer knee bolster configuration for Test 2. Between the first and second tests, the deformed knee bolster from the first test was cut out from the desk at both top and bottom connections, and a new knee bolster was welded into place. Additionally, the bottom edge of the desk, where the knee bolster connects, had to be repaired to mend some damage from the first test. Detailed review of the test articles after the test indicated that those repairs resulted in a stiffer bottom connection than originally intended. To account for this stiffer connection, the post-test knee bolster model was stiffened as outlined earlier. Figure 26 compares the femur load curves; it is evident that the stiffening introduced in the post-test model helps to improve the correlation, resulting in a time history that is similar to the test result, without negatively affecting ATD kinematics.

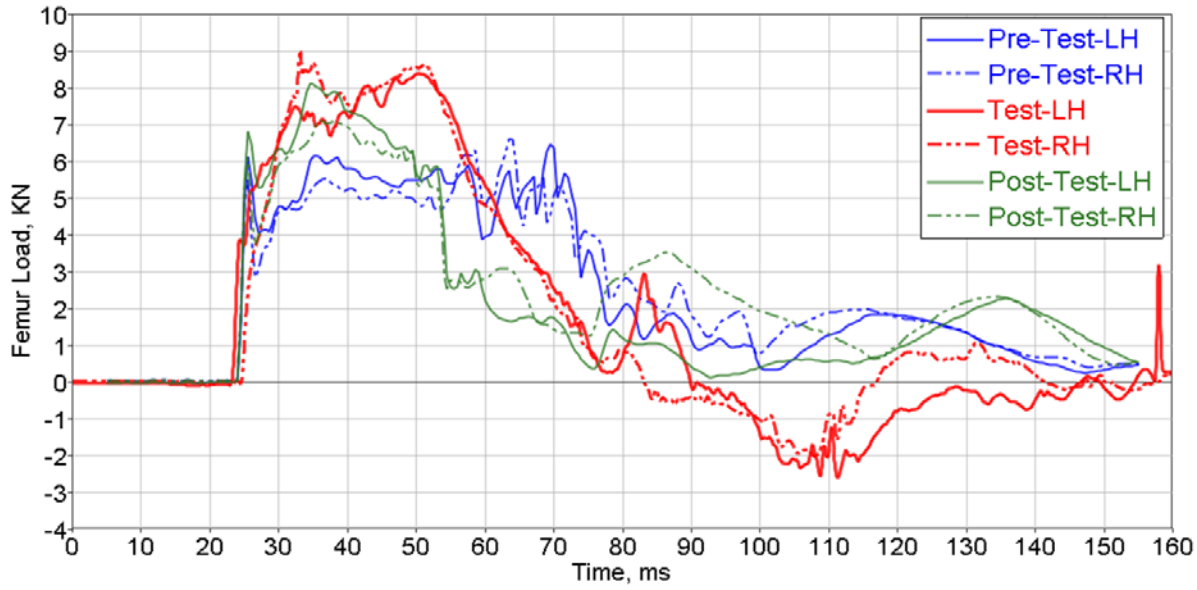

Figure 26. Comparison of Femur Loads

5.5 Neck Injury Indices

Figure 27 presents the neck forces, neck moments, and the neck injury indices for the simulations and the tests. In general, there is good correlation between the simulation results and the test results, particularly the post-test simulations, though no specific steps were taken to improve the correlation for the neck indices. The improvements observed are the result of updating parameters to improve overall correlation, particularly the head accelerations. The neck forces in the X-direction match especially well in the post-test model. For forces in the Z direction, the two simulations and the test are fairly similar, though, much like the head acceleration curves, the simulations indicate an early spike (at about 55 ms) that is not seen in the test. For the neck flexion-extension moment (Y-direction), the post-test simulation shows good

similarity to the test data in the negative portion of the curve, with the rise on the positive side being offset in time.

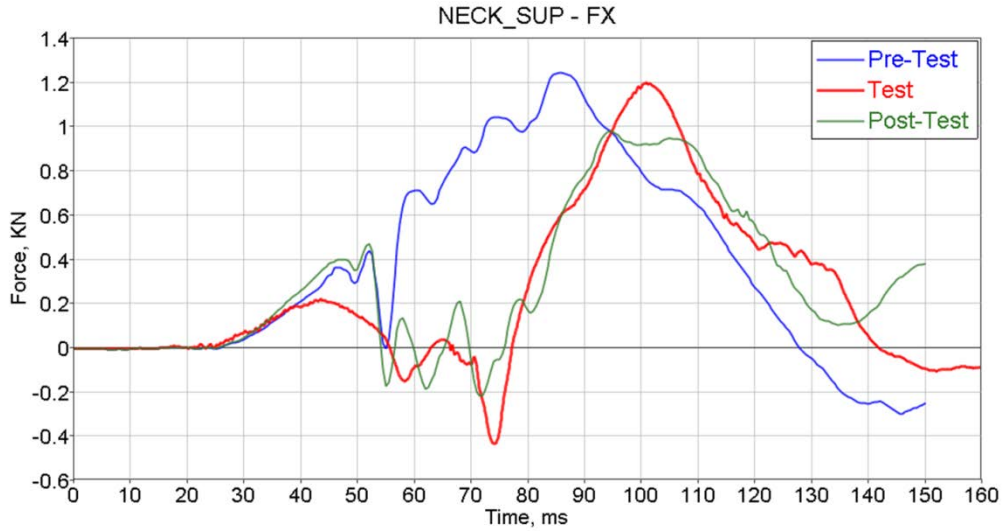

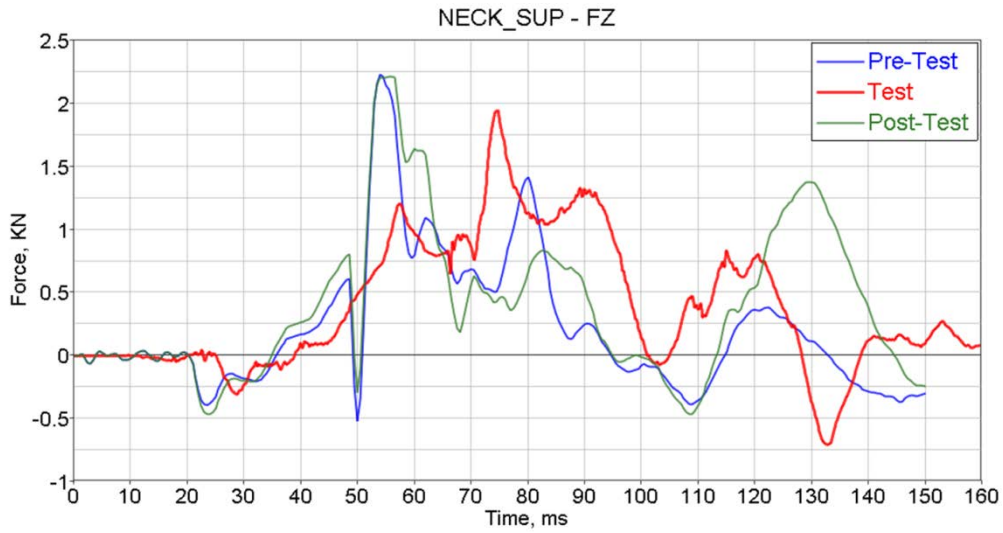

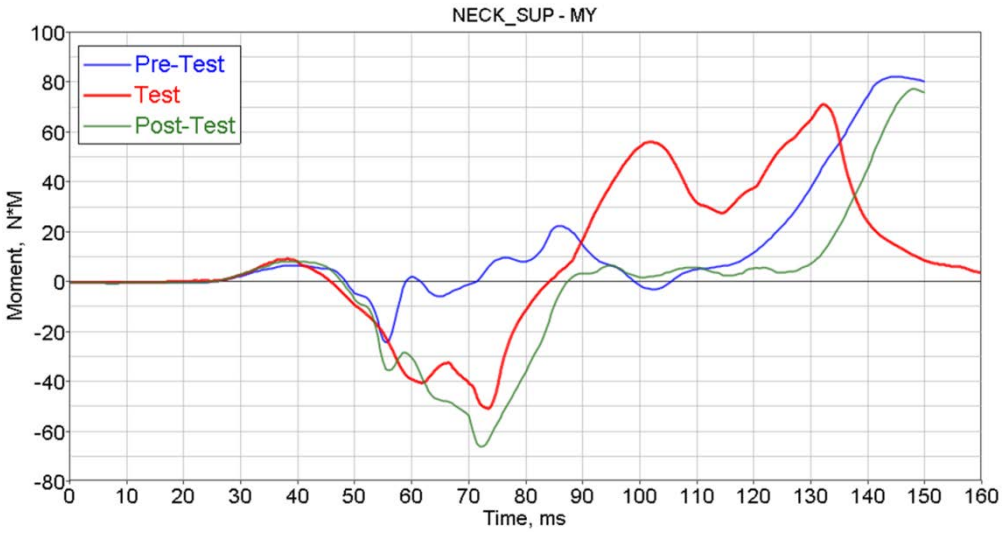

Figure 27. Comparison of Neck Forces and Moments

5.6 Summary

The simulations presented have captured the ATD kinematics, forces, moments, and injury indices with sufficient fidelity to serve as an effective tool for designing similar protection systems. In fact, most differences observed between the simulations and the test data would likely fall within the expected range of statistical variations in design, manufacturing, and ATD setup, thereby adding confidence to the development effort.

6. Conclusions and Recommendations

Performance of a prototype EPS for cab car engineers, consisting of an airbag system and a deformable knee bolster system, was successfully demonstrated under simulated collision conditions, using dynamic sled tests. The tests highlighted the ability of the EPS to protect a cab car engineer in a moderate-to-severe train collision, meeting all prescribed criteria, including compartmentalization, limits of injury to the head, neck, chest, and femur, and continuing to meet all functional requirements. The system functions without requiring input from the engineer, without restraining him or her, and without impeding egress, while adding only minimally to cost or weight of the car.

As part of this phase, SA constructed:

- a baseline cab desk, which would serve as the test bed for the EPS;
- the airbag subsystem, comprised of an airbag and an inflator; and
- the knee bolster subsystem, comprised of deformable brackets and honeycomb blocks.

The EPS subsystems were then assembled into the baseline cab desk, and the full system was dynamically tested under a 23G EPS test pulse to demonstrate compliance with the injury criteria and compartmentalization requirements.

Critically, the project demonstrated the feasibility of developing a protection system that can effectively protect engineers under moderate-to-severe collision conditions, using modern occupant protection concepts and technologies.

Based on the success of this prototype effort, we recommend the following:

- The current effort focused on minimizing injuries to the head, neck, chest, and femur. Abdominal protection is another safety element that has been drawing attention recently. During this effort, we observed, albeit qualitatively, that the prototype EPS protected the abdomen reasonably well, but this was not quantified. In the next phase of the effort, it would be useful to include an abdominal performance target and tailor the system to meet those requirements. It may also be worthwhile to include the tibia injury criterion.
- The prototype system worked effectively under the prescribed ATD and test conditions; for example, with a 95^{th} percentile male ATD. To extend and ensure the viability of such a design, it is essential to verify that the system works as intended under a variety of ATD sizes (50^{th} percentile female, for example), ATD positions, and test pulses. Therefore, we recommend the verification of system performance under a varied test matrix, first analytically, and then through physical testing, including making any revisions deemed necessary to the conceptual design to ensure that the range of protection remains broad.
- Based on the lessons learned so far, as well as feedback from end users, the system could be optimized for better performance and better ergonomics. For example, there are opportunities to simplify the design further and improve the cost-effectiveness of the design from material and manufacturing perspectives. We recommend that an updated system incorporating the lessons learned be designed, fabricated, and demonstrated to industry, highlighting the critical design elements and potential safety benefits.

- Trigger threshold values and associated time delays/gaps are specific to each car design and were therefore not explored in great detail for this project. We recommend initiating a research project that simulates the crush behavior of a modern car design under a variety of impact conditions, as well as gathering data from past impact tests to prepare detailed guidelines on trigger design based on those simulations and test results.
- Based on the results of this project, the FRA is interested in studying the applicability of this technique to locomotives. We recommend studying this option further and conducting an appropriate demonstration.

7. References

1. Prabhakaran, A., Singh, S.P., and Vithani, A.R., "Prototype Design of a Collision Protection System for Cab Car Engineers," Report to FRA, Report No. DOT/FRA/ORD-13/15, March 2013.
2. Severson, K., Parent, D., "Train-to-Train Impact Test of Crash Energy Management Passenger Rail Equipment: Occupant Experiments," American Society of Mechanical Engineers, Paper No. IMECE2006-14420, November 2006.
3. Priante, M. "Review of a Single Car Test of Multi-Level Passenger Equipment," American Society of Mechanical Engineers, Paper No. JRC2008-63053, April 2008.
4. Muhlanger, M.P., Severson, K., Perlman, B., Prabhakaran, A., Singh, S.P., and Vithani, A.R., "Prototype Design of an Engineer Collision Protection System," Paper JRC 2012-74073, ASME Joint Rail Conference, April 10–18, 2012, Philadelphia, PA.
5. Code of Federal Regulations, Title 49, Part 571, Section 208, Occupant Crash Protection, October 1, 2002.
6. Radioss, Version 10, Altair Hyperworks, Troy, MI.
7. SAE International, Aerospace Standard AS8049, 1997.

Appendix A.
Comparison of Airbag Deployment Sequences—Static Deployment

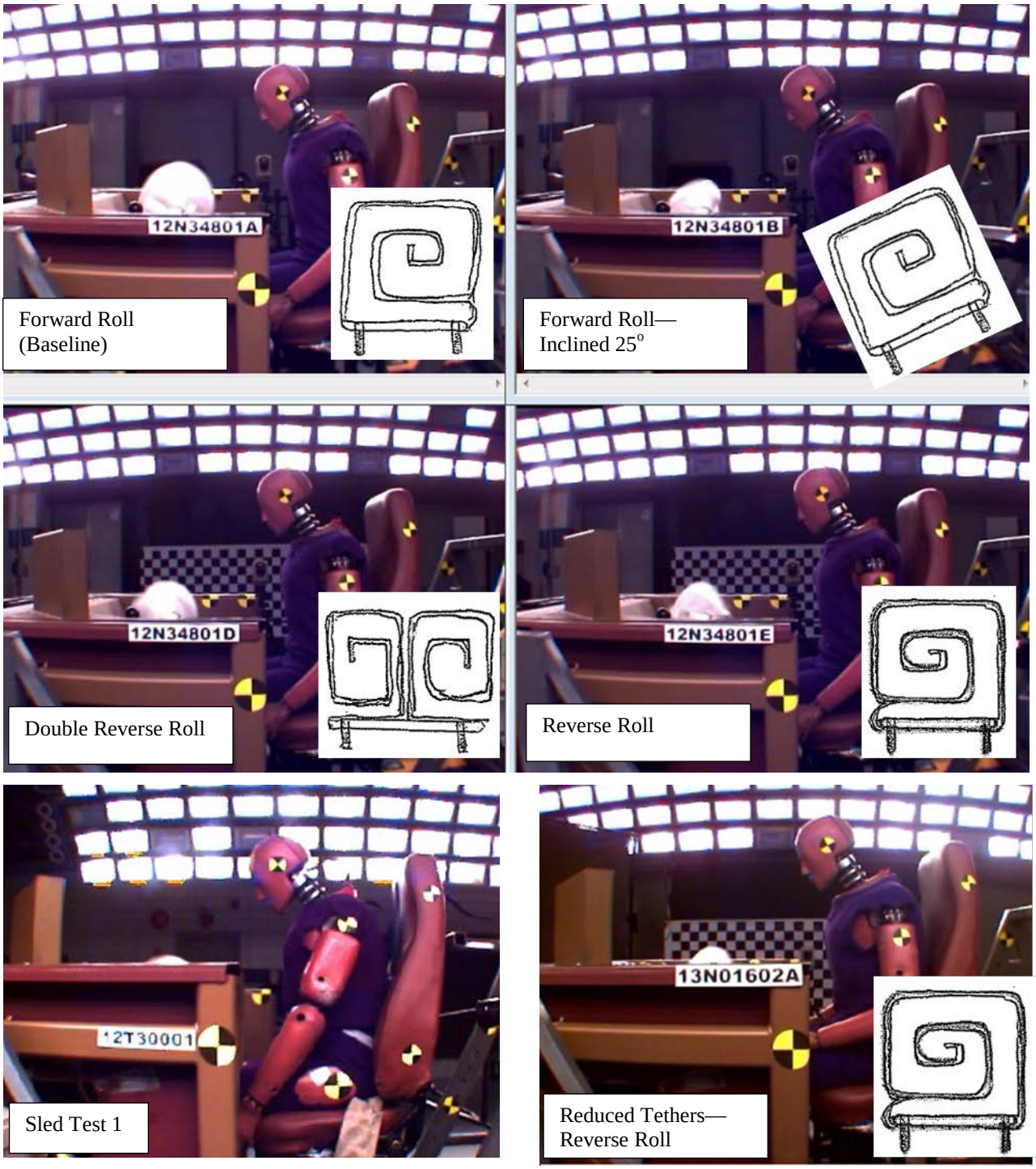

Figure A1. Deployment Sequence—Static Deployment Tests, t = 10 ms

Figure A2. Deployment Sequence—Static Deployment Tests, t = 15 ms

Figure A3. Deployment Sequence—Static Deployment Tests, t = 20 ms

Figure A4. Deployment Sequence—Static Deployment Tests, t = 25 ms

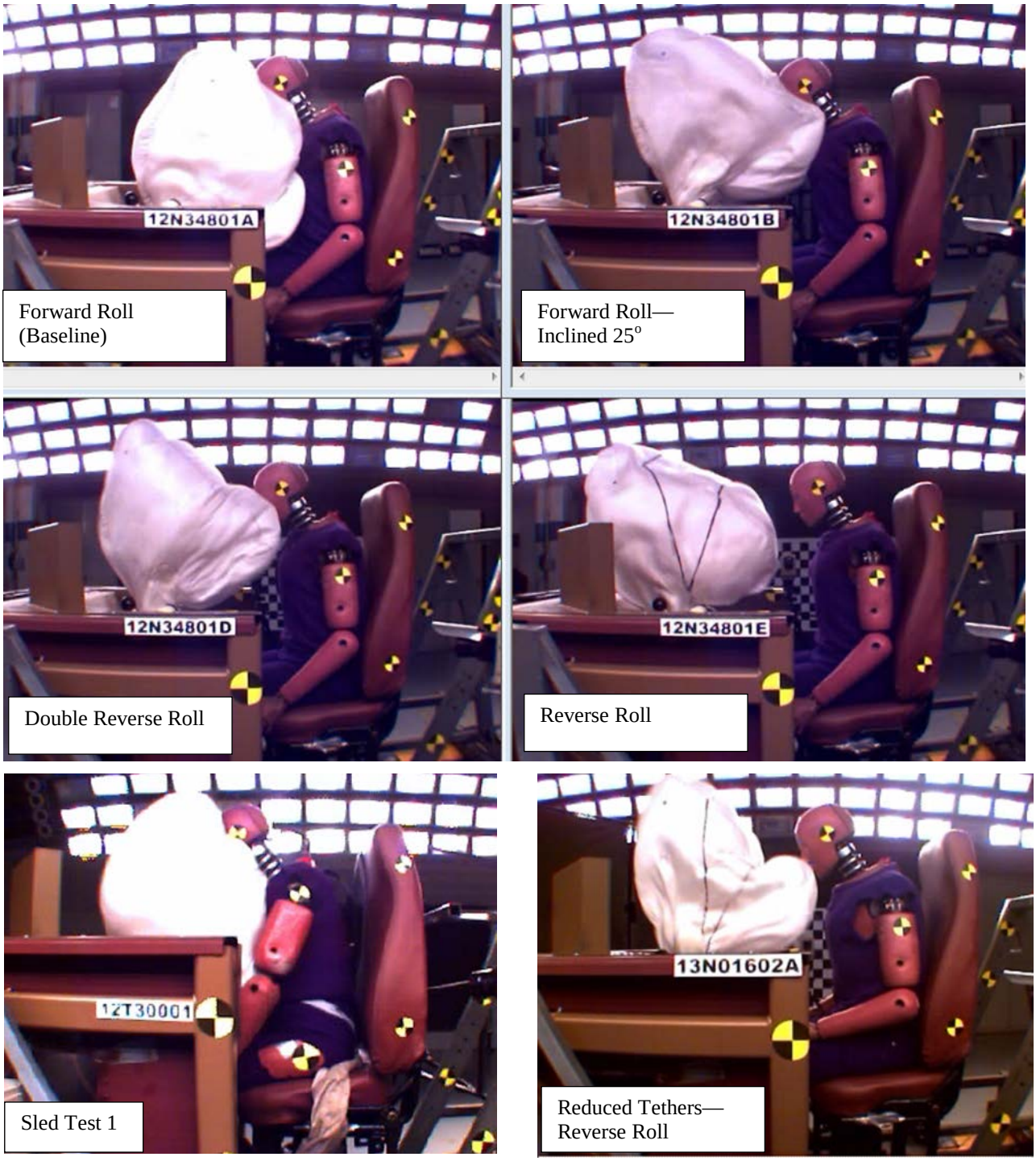

Figure A5. Deployment Sequence—Static Deployment Tests, t = 30 ms

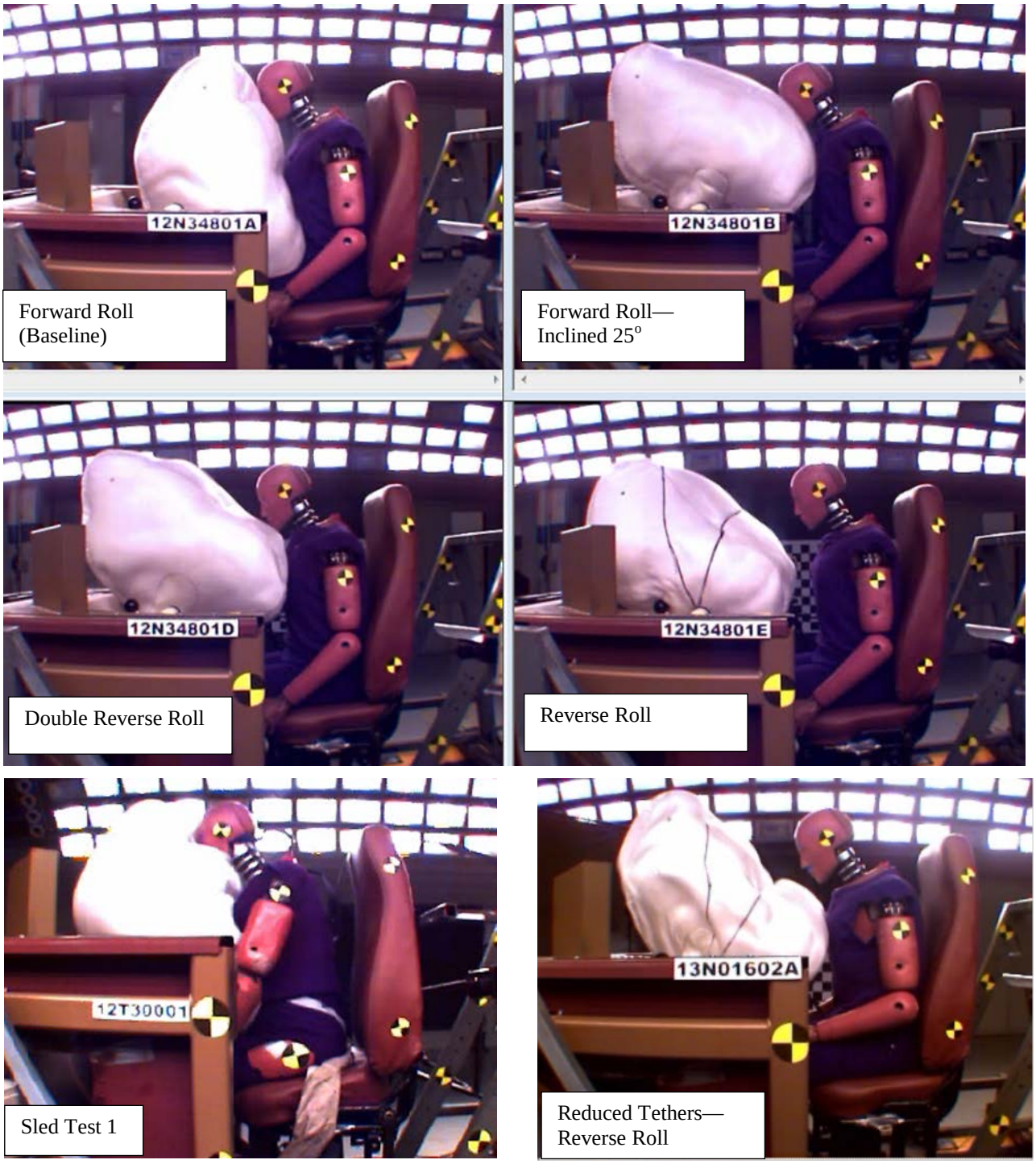

Figure A6. Deployment Sequence—Static Deployment Tests, t = 35 ms

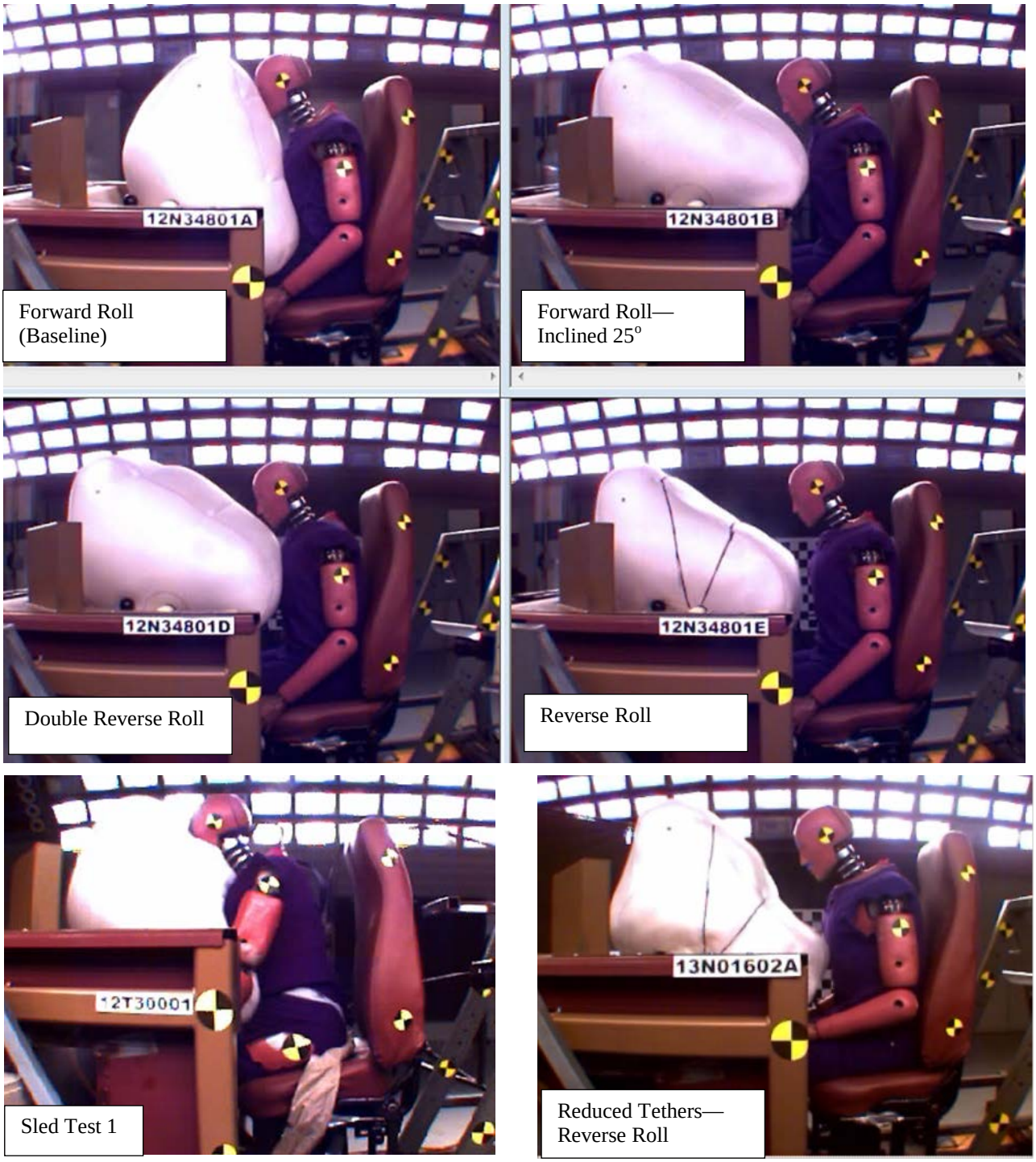

Figure A7. Deployment Sequence—Static Deployment Tests, t = 40 ms

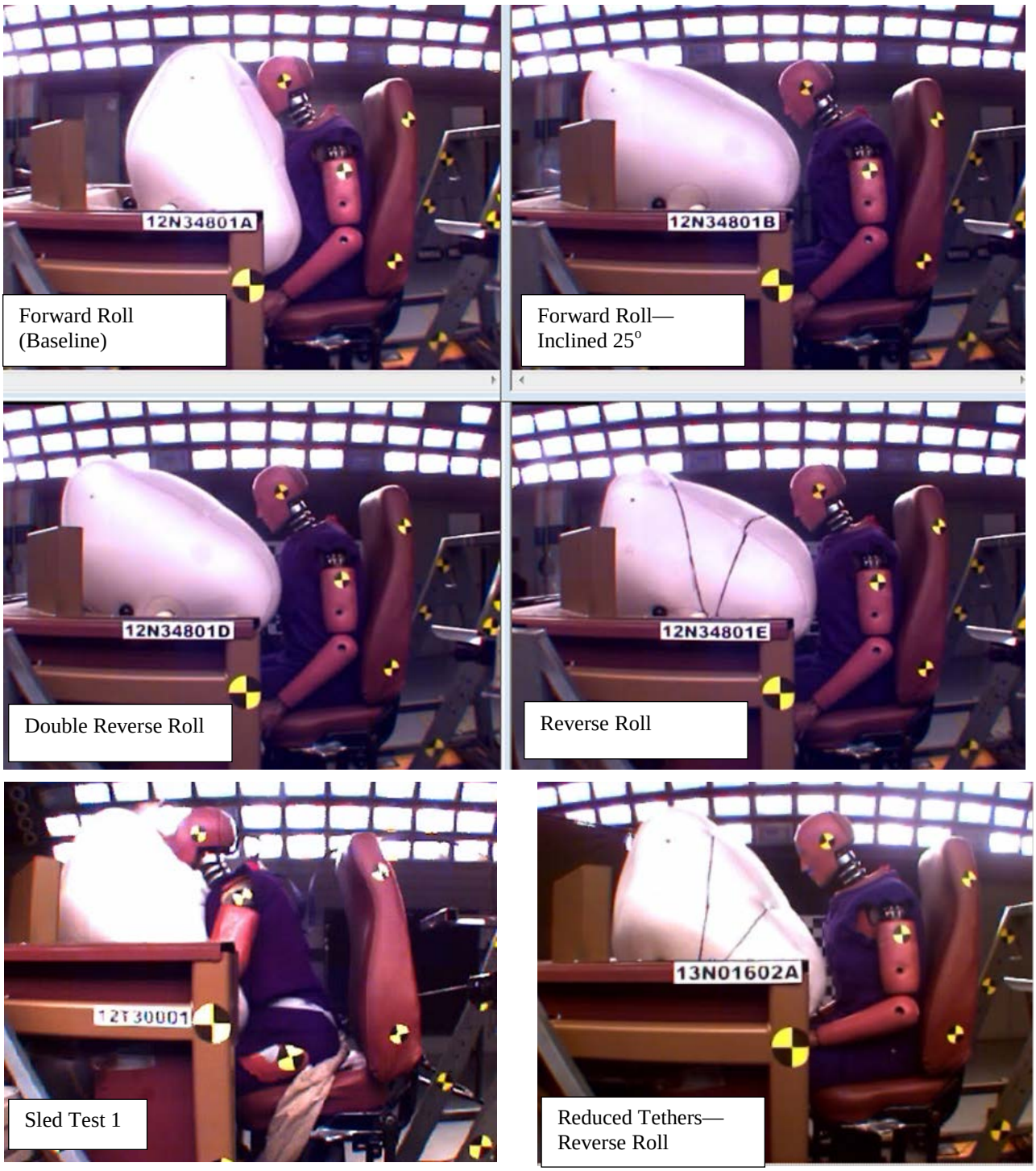

Figure A8. Deployment Sequence—Static Deployment Tests, t = 45 ms

Abbreviations and Acronyms

ADC	Analog-to-Digital Conversion
ATD	Anthropomorphic Test Device
CFR	Code of Federal Regulations
DAS	Data Acquisition System
EPS	Engineer Protection System
FRA	Federal Railroad Administration
FMVSS	Federal Motor Vehicle Safety Standards
HIC_{15}	Head Injury Criterion (15 ms)
KSS	Key Safety Systems
N_{ce}	Neck Injury Index (compression-extension)
N_{cf}	Neck Injury Index (compression-flexion)
N_{te}	Neck Injury Index (tension-extension)
N_{tf}	Neck Injury Index (tension-flexion)
SA	Sharma & Associates, Inc.